SMART ANTENNA PATTERN BEAMFORMING IN THE DESIGN OF MODULATION, CODING AND MULTIPLE ACCESS TECHNIQUES

by

SM Javad Hoseyni

Submitted in partial fulfillment of the
requirements for the degree of Doctor of Philosophy

at

Dalhousie University
Halifax, Nova Scotia
August 2019

Dedicated to my lovely wife, Jila,

my amazing children; Arazoo and Zahed,

as well as my supportive parents; Khales and Ferdous.

Contents

List of Figures

List of Abbreviations and Symbols Used

The list of abbreviations and acronyms used in this dissertation are as follows:

3D	Three Dimentions
GSM	Global System For Mobile Communications
QAM	Quadrature Amplitude Modulation
SISO	Single Input Single Output
SNR	Signal To Noise Ratio
5G	Fifth Generation
AOA	Angle Of Arrivals
AOD	Angle Of Departure
APM	Amplitude And Phase Modulated
APM	Amplitude And Phase Modulation
AWGN	Additive White Gaussian Noise
BACM	Beam Angle Channel Modulation
BAMA	Beam Angle Multiple Access
BASK	Beam Angle Shift Keying
BER	Bit Error Rate
BPSK	Binary Phase Shift Keying
BS	Base Station
BSVM	Beam Steering Vector Mapper
CDMA	Code Division Multiple Access
CW	Continuous Wave
DM	Detection Matrix
DOA	Direction Of Arrival
DOD	Direction Of Departure
DOD	Direction Of Departure
FDMA	Frequency Devision Multiple Access

G-BACM	Generalized Bacm
i.i.d	Independently And Identically Distributed
IM	Index Modulation
LOS	Line Of Sight
MIMO	Multiple Input Multiple Output
MISO	Multiple Input Single Output
ML	Maximum Likelihood
MCR	Maximal Correlation Receiver
MRC	Maximal Ratio Combining
MUSIC	Multiple Signal ClassifiCation
NLOS	Non Line Of Sight
O-STBC	Orthogonal Space Time Block Codes
PIMRC	Personal, Indoor And Mobile Radio Communications
PSD	Power Spectral Density
PSK	Phase Shift Keying
RF	Radio Frequency
RV	Random Variable
SDMA	Space Division Multiple Access
SDMA	Spatial Division Multiple Access
SER	Symbol Error Rate
SIMO	Single Input Multiple Output
SM	Spatial Modulation
SSK	Spatial Shift Keying
STBC	Space Time Block Coding
TDMA	Time Division Multiple Access
ULA	Uniform Linear Array
VAOA	Virtual Angle of Arrival
VTC	Vehicular Technology Conference
WD	Wireless Days

The list of symbols used in this dissertation are as follows where bold-face letters

denote matrices and vectors also, scalar variables are in plain lower-scale letters.

$\|\cdot\|$	L_2 norm of a vector
$(.)^H$	Hermitian transpose
$(.)^T$	matrix transpose
α	phase propagation factor
θ_k	k^{th} AOD
θ_v	virtual angle or virtual delay
θ_i	delay associated with the angle-of-arrival (AOA) φ_i
λ	carrier wavelength
φ_k	k^{th} AOA
B_w	passband transmission bandwidth
d	ULA elements spacing
d_{ij}	inter distance between symbol i and j
d_{min}	minimum Euclidian distance between the constellation points
$\mathbf{D}$	correlation matrix
$\mathrm{erfc}(\cdot)$	standard error function complementary
M	total number of beams for all users
M_i	number of symbols/beams for user i
M_{min}	points in the constellation with minimum distance
$\mathbf{N}$	noise vector
N	number of users
n_i	scalar AWGN at the i-th antenna
N_0	the noise power spectral density (PSD)
N_r	number of receive antennas
N_t	number of transmit antennas
$\Re(\cdot)$	real part
R_b	data rate
$S(t)$	APM signal
$\mathbf{W}_i$	weight vector
w_i^n	n^{th} complex coordinates of $\mathbf{W}_i$

Acknowledgements

Abstract

Smart antenna systems hold promise to meet the projected demand for increased channel capacity in future wireless communications services. This dissertation is concerned with the design of Index Modulation (IM) algorithms based on switched beam antenna systems, which benefit from energy efficiency of the antenna array gain, in addition to improved spectral efficiency. In this research, the latter is accomplished through transmitting spatial streams by indexing beams representing the directions of signal arrival. In particular, this dissertation develops a common framework based on beamforming patterns for the design of modulation, coding, and multiple access techniques.

First, this dissertation contributes three schemes that embed information in the radiated beam patterns. As a starting point, beam angle shift keying (BASK) is introduced, where a spatial symbol selects a single active beam for the unmodulated carrier signal. This scheme is then extended to beam angle channel modulation (BACM), where in addition to a spatial stream, an amplitude and phase modulated (APM) carrier signal is considered. Finally, a generalized BACM (G-BACM) is devised, where the spatial symbol selects two or more simultaneously transmitted beams. In all these modulation schemes, when the transmitter selects one of the M_s beamforming patterns, this increases the spectral efficiency of a spatial stream by $\log_2(M_s)$. A key point is that M_s can be much larger than the number of antennas. This contrasts with traditional multiple-input multiple-output (MIMO) systems, where the increase in spectral efficiency is governed by the minimum number of transmit and receive antennas.

Secondly, this dissertation extends BASK modulation into a multi-user version referred to as beam angle multiple access (BAMA). Specifically, multiple access on the uplink is achieved by assigning subsets of beams to individual users signaling with BASK. At the base station, over the duration of the spatial symbol, the receiver decides on a subset of possible multiple angles of arrival (AOA) corresponding to spatial symbols from different users.

Thirdly, this dissertation proposes a multibeam version of space-time block coding (STBC). By utilizing simultaneous transmissions of two or more beams in G-BACM, this work introduces diversity for the QAM/PSK symbols and increases the reliability of the spatial (beam angle) symbols by providing replicas for the group of beam angle signatures (repetition coding).

This dissertation advances efficient spectrum and power utilization in wireless transceivers by exploiting beamforming pattern switching in smart antenna systems. The motivation behind this work is to allow future wireless transceivers operating at higher frequencies to combat high signal attenuation through digital beamforming.

1   Introduction

Due to the ever-growing demand for wireless communication systems that support higher bit rates and a higher quality of service despite being restricted by spectrum scarcity, there is continuing pressure to increase the spectral efficiency of new signaling schemes. Advanced antenna systems with multiple-input multiple-output (MIMO) technologies are crucial building blocks for improving the capacity of present and future wireless networks [1] − [3]. The MIMO designs offer different ways of improving the performance of communication systems, through (i) spatial multiplexing and diversity, as well as (ii) smart antenna array (beamforming) gains [4], [5]. There are two fundamental approaches in standard MIMO networks using antenna arrays. These involve the parallel transmission of independent data streams to maximize the spatial multiplexing gain, and space-time coding to maximize the diversity gain (reliability) [6]. In contrast, beamforming is a robust technique which spatially focuses power toward the target receiver and reduces interference to and from other directions [7]. Beamforming is accomplished through the manipulation of signals induced in various antenna elements. This array signal processing, with adaptive algorithms to adjust the required antenna weighting, is exploited in this dissertation to advance the design of wireless communication signaling schemes such as modulation, coding and multiple access [8].

As technology moves toward fifth-generation (5G) mobile communications, the

concepts of MIMO are evolving to include massive MIMO and coordinated multi-point transmission [9]. However, alternative advanced MIMO schemes that reduce the number of RF chains required and permit the use of compact antennas are being considered for wireless communications beyond 5G [10]. This stems from the fact that, to overcome today's spectrum scarcity in traditional frequency bands, new spectrum opportunities are also being explored, particularly in the millimeter-wave (mmWave) frequency bands [11]. Operating at higher frequencies, above 6 GHz, implies greater attenuation as well as different implementation challenges than is the case with standard approaches. This is the reason why, in this dissertation, an advanced antenna solution that can also benefit from smart antenna array advantages in the mmWave band is pursued [12]. Furthermore, the proposed system model also attempts to benefit from non-line-of-sight (NLOS) directional communication, which has already been exploited for fixed wireless backhaul/outdoor communication in these frequency bands.

To address the requirements of future wireless communication systems with enhanced throughput and quality of service, this dissertation introduces new signaling schemes for point-to-point wireless links that (i) increase spectral efficiency, and (ii) benefit from antenna array gains. Specifically, these techniques take advantage of multiple specular reflection paths between the transmitter and receiver. By activating one of the beams (or a subset of such beams) at the transmitter by using phased antenna arrays, and via indexing of the transmitting beam(s), the transmission of spatial symbols is accommodated. This increases bandwidth efficiency beyond what would usually be transmitted via amplitude and phase modulation (APM) symbols alone. This beamforming pattern based modulation is investigated for different configurations of beams, antennas, concatenation with APM, and space-time block coding (STBC), thus offering flexibility when balancing the complexity of the signaling scheme and its performance. The proposed modulation is also extended from

single-user to multiuser transmissions, where similarly, as in space-division multiple access (SDMA), antenna arrays are employed at user terminals to steer the carrier signal toward the base station (BS), however users change the beam patterns depending upon the transmitted data.

The adaptive steering of multiple beams to send data has already been used for some time in the context of SDMA, when implementing multiple access for different users through virtual channels in the angle domain [13]. However, in this dissertation, multiple beams (or rather beam patterns) are initially exploited to transmit data for one transmitter-receiver connection, to increase the data rate beyond that of conventional APM transmission. Only then is this approach analyzed in the context of multiple access. The unique feature of transmitting "spatial" data through beam indexing breaks away from the traditional operation of SDMA, where data of one transmitter-receiver pair is sent on one beam only. The signaling schemes developed in this dissertation are more in line with a general concept of index (or permutation) modulation where, in addition to APM symbols, other data are sent through channel indexing, as in spatial modulation (SM) where the transmitting antennas are indexed [14]. In this work, by indexing beams or beam patterns and mapping the input bits on a selected permutation of the beam set, increased data rates can be achieved through low-complexity implementations of multiple beams with smart antennas.

1.1 Dissertation Objectives, Contributions and Organization

1.1.1 Objectives

The general objective of this dissertation is to exploit smart antenna array advantages (e.g., beamforming and nulling) when designing various signaling schemes, by adaptively switching antenna radiation patterns. To this end, multi-antenna transmission schemes are developed that can realize the benefits of conventional MIMO communications by performing the modulation process at the RF stage of the transmitter [3]. These schemes depend (i) on the information-driven beam pattern switching mechanism (during the encoding phase), and (ii) on the separability of the transmitter-to-receiver beams (during the decoding phase). This is in contrast to traditional beamforming approaches where, when taking advantage of the antenna gain, only one direction is used at the transmitter to send APM symbols on the carrier signal.

This dissertation develops a novel transmission technique that uses an antenna array to encode information symbols in the angle of propagation (and arrival) wave of the wireless channel. At the encoder, the block of information bits is mapped into two symbols: (i) a spatial symbol selecting the direction of arrival of the amplitude- and phase-modulated carrier signal, and (ii) a temporal symbol chosen from the constellation diagram, such as quadrature amplitude modulation (QAM) or phase shift keying (PSK). The proposed scheme follows the model for concatenated modulation designs, as in the recently introduced spatial modulation (SM) approach. Specifically, this approach attempts to exploit the indices of the transmitting beams as a signaling dimension for transmitting spatial symbols. This is in addition to employing the traditional temporal signaling dimensions using QAM or PSK [15], [16]. The benefit of

this scheme is that it requires only a subset of RF chains (as few as one), as compared with conventional MIMO systems.

The proposed spatial signaling through beamforming indexes provides a framework for studying the adaptive antenna transmissions technique in single and multiple user scenarios. The originally proposed single beam based index modulation, referred to as beam angle channel modulation (BACM), is generalized to map the spatial symbol to the index representing the active subset of possible beams. The primary advantage of this generalized beamforming and pattern selection based modulation is that it allows APM signals to be transmitted on parallel active beams. This scheme is also investigated when employing STBC to combat fading channels and when trading off between the system data rate and reliability. As in SDMA, when deploying the proposed modulation in multiuser scenarios, antenna arrays are employed at the user terminals to steer the carrier signal toward the BS, however, users change the beam patterns depending upon the transmitted data. At the BS, an adaptive antenna system is used to decide on the directions of simultaneous single-carrier signals in the same band, characterizing different users.

Generalized BACM allows the spatial symbol at the transmitter to select a beam pattern with two or more active beams. In a single channel use, the transmitted information is conveyed (i) in spatial symbols indexing the activated combination of K simultaneous transmit/receive beams, and (ii) in the K APM symbols from QAM/PSK constellations. The K APM symbol streams are transmitted in parallel on the K active beams. Working with combinations of K active beams (of the total number of N_B potential beams generated in the transmit antenna array) increases the spatial modulation level in G-BACM.

In beam angle multiple access (BAMA), an interference-aware multiuser detection technique is developed to accommodate a multiuser communication scenario. Multiple access in the system is attained by assigning subsets of beams to individual users

signaling with BASK. At the base station, for the duration of the spatial symbol, the receiver decides on a subset of possible multiple angles of arrival (AOA) corresponding to synchronized spatial symbols from different users. Unlike the situation in SDMA, where a fixed beam arrangement is used, BAMA detects the beams employed by several users on a symbol-by-symbol basis.

In this dissertation, due to the system and algorithm complexity, it was not feasible to use only analytical methods to evaluate the performance of the algorithms developed or to pursue practical implementations. Therefore, a combination of analytical and simulation results is employed. All proposed schemes and algorithms have been validated and compared through a large number of computer simulations run in the $MATLAB^{\circledR}$ computing environment. In this area of research, this is an acceptable research methodology for solving wireless communication problems and arriving at new knowledge and designs.

This dissertation contributes to the theoretical development of a new spatial modulation technique, with the extensions for other aspects of communication systems like coding and multiple access. The results are verified through simulations. This is the first step, which precedes practical implementation. This is an acceptable methodology in the field of communication system design, since not all physical layer wireless communication proposals proceed to the implementation stage.

1.1.2 Contributions

Results of the research described in this dissertation have been published in the form of conference papers in [17] – [20]. In addition, one journal article is in preparation. The details of these publications are outlined below.

Refereed Conference Proceeding Publications

[C-1] **J. Hoseyni** and J. Ilow, "*M-ary Beam Angle Shift Keying Modulation for*

MIMO Channels," in 2018 Wireless Days (WD), 3-5 April 2018, pp. 190-195.

[C-2] **J. Hoseyni** and J. Ilow, "*Beam Angle Channel Modulation*," in 2017 IEEE Vehicular Technology Conference (VTC Fall), 24-27 September 2017.

[C-3] **J. Hoseyni** and J. Ilow, "*A Novel Multiple Access Technique Based on Antenna Radiation Pattern Modulation*," in 2018 IEEE 29th Annual International Symposium on Personal, Indoor and Mobile Radio Communications (PIMRC), 9-12 September 2018, pp. 1447-1452.

[C-4] **J. Hoseyni** and J. Ilow, "*Generalized Beam Angle Channel Modulation with Space-Time Block Coding*," in 2019 IEEE 90th Vehicular Technology Conference: VTC2019-Fall, 22-25 September 2019.

Journal Papers (in preparation)

[IPJ-1] **J. Hoseyni** and J. Ilow, "*Generalized Beam Angle Channel Modulation*," to be submitted to Wireless Communications.

The research in each of the papers cited above was initiated and carried out by the principal author of the papers, who is also the author of this dissertation.

The research contributions of this dissertation can be classified into four areas, which correspond to the four main chapters of the dissertation. The chapters and the specific papers that relate to them are listed below.

Chapter 2: **Radiation Pattern Beam Angle Shift Keying**

A new beamforming based modulation technique is introduced, referred to as beam angle shift keying (BASK) modulation. It uses an antenna array to encode information symbols in the angle of wave propagation (and arrival) in a multiple-input multiple-output (MIMO) wireless channel. Specifically, at the transmitter, the block of information bits is mapped into a "spatial" symbol

selecting the beam, or equivalently the direction of departure (DOD), for the unmodulated carrier signal. [C-1].

Chapter 3: **Two Layer Data Encoding Communication System**

A concatenated 3D modulation is proposed, where the block of information bits is mapped into two symbols: (i) a spatial symbol selecting the direction of arrival of the amplitude and phase modulated carrier signal, and (ii) a temporal symbol chosen from a constellation diagram such as QAM or PSK. [C-1] and [C-2].

Chapter 4: **Multiple Access Technique Based on Beam Angle Shift Keying**

An interference-aware multiple access technique is developed. This unique multiuser transmission scheme employs multiple beam patterns to communicate with multiple users on a single carrier. [C-3] and [IPJ-1].

Chapter 5: **Generalized Beam Angle Channel Modulation with Space-Time Block Coding**

Generalized BACM allows the spatial symbol at the transmitter to select a beam pattern with two or more active beams instead of a single beam for any channel. This provides greater spatial bandwidth efficiency than is the case with BACM. In addition, a multibeam STBC is developed to introduce diversity for the QAM/PSK symbols and to increase the reliability of the spatial (beam angle) symbols by providing replicas for the group of beam angles signatures (repetition coding). [C-4] and [IPJ-1].

1.1.3 Organization

This dissertation is organized into six chapters. The first chapter outlines the objectives, contributions, and dissertation organization, as well as the general concepts

and models used throughout the dissertation. The last chapter contains the conclusions and offers suggestions for future work that could be carried out to expand upon the results.

Chapter 2 discusses the new application of beamforming. A new modulation technique is introduced which encodes data in the beam angle of the power radiated in the wireless channel. This is referred to as beam angle shift keying (BASK).

Chapter 3 focuses on extending the proposed BASK technique to a concatenated 3D modulation scheme referred to as beam angle channel modulation (BACM). In addition to encoding information bits in the angle of the transmitting beam, BACM also includes conventional QAM or PSK on the RF carrier.

In Chapter 4, by extending the BACM modulation scheme to a multiuser scenario on the uplink, an interference-aware multiuser detection technique is developed, which is referred to as beam angle multiple access (BAMA).

In Chapter 5, generalized BACM is introduced, first to allow the spatial symbol at the transmitter to select a beam pattern with two or more active beams. This is referred to as G-BACM. Space-time block coding is then proposed, (i) to transmit multiple copies of data streams across a number of beams and time slots, and (ii) to exploit the various versions of the data received to improve the reliability of data transfer.

The remainder of this chapter provides a review of concepts and literature in relation to the research pursued in this dissertation. Specifically, Sections 1.2 and 1.3 present the building blocks related to the research in more detail and review the corresponding literature in the areas of (i) communication systems overview, (ii) bandwidth efficiency, (iii) space-time block coding, (iv) multiple access with SDMA, and (v) antenna arrays.

1.2   Communication Systems Overview

Generally, communication involves the transmission of information from a source to a destination through a series of operations. Regardless of the form of communication being considered, every communication system has three fundamental elements: a transmitter, a channel, and a receiver [4], each with a specific role, as shown in Figure 1.1. The primary communication process in every wireless system is data encoding or modulation [16].

Digital systems employ sophisticated modulation techniques to increase spectrum efficiency by combining multiple bit transmissions into signal representations, using a nominal one hertz of bandwidth. For example, 8-ary quadrature amplitude modulation (QAM) defines a total of eight possible combinations of amplitude and phase, which permits three bits to be encoded in one hertz of bandwidth in a conventional single-input single-output (SISO) transceiver. The following section is devoted to a review of data encoding techniques, and also examines some of the wireless communication concepts used in this dissertation.
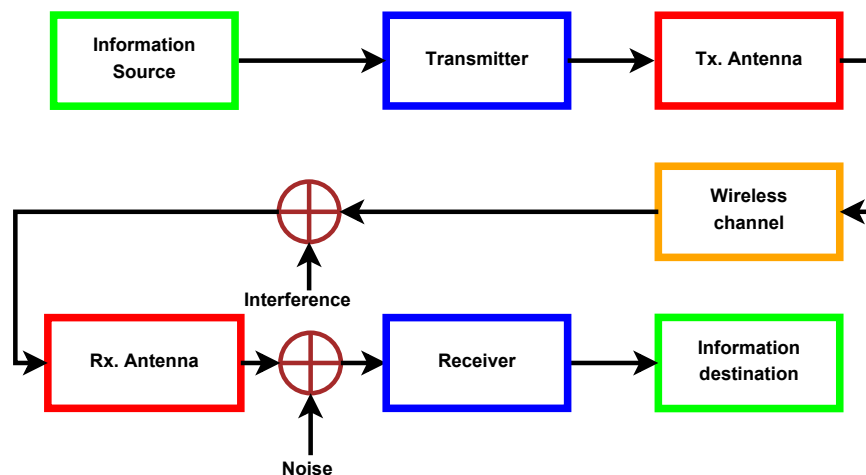
Figure 1.1: Wireless communication system.

1.2.1 Data Encoding Techniques

In communication systems, modulation is the act of changing a signal to transmit useful data and matching this signal to a channel medium within a particular spectral bandwidth [21]. A source message is usually represented initially by a baseband signal, commonly referred to as an information bearing signal. This signal varies one or more of three parameters: amplitude, phase, and frequency of the radio frequency (RF) carrier signal. In this way the baseband signal is carried by the modulated carrier through a wireless channel from the transmitter to the receiver. Among traditional digital modulation schemes, QAM is attractive, with applications in many advanced communication systems, due to the efficient use of bandwidth and hardware [22].

Recently, index modulation (IM) techniques are attracting more interest [23], [24]. In IM, transmit entities other than amplitudes/frequency/phases are used to convey information. Some of these schemes exploit an antenna or subcarrier index to encode the information while others, such as media-based modulation (MBM), embed information in variations of the transmission media (channel states) [25]. Specifically, there is an interest in designing multi-antenna transmission schemes that can realize the benefits of MIMO communications, i.e., spatial multiplexing and transmit/receive diversity, by performing the modulation process at the RF stage of the transmitter, rather than using baseband modulation [26]. In this area, two multi-antenna transmission algorithms have attracted considerable attention in the MIMO literature due to the reduced complexity of their structure: (i) spatial shift keying (SSK) [27], [28], and (ii) spatial modulation (SM) [29], [30]. SSK exploits transmit antenna indices as the information source and uses the distinct multipath characteristics of different antennas to differentiate between the spatial symbols transmitted. SM, which is a concatenation of SSK and amplitude/phase modulation, e.g., QAM, can offer better

performance than conventional MIMO schemes and a reduction in transceiver complexity, e.g., a single RF chain [31]. For review purposes, these modulation schemes are described below.

QAM Modulation

Conventionally, when data is encoded into the amplitude and phase of a carrier signal, the "temporal" symbols are represented by using QAM or PSK [15], [16], [32]. The 16-QAM system yields sixteen distinct signal states, as illustrated in the signal constellation graph in Figure 1.2. Thereby, each signal impulse, or symbol, carries one of sixteen possible signal combinations and represents four bits ($2^4 = 16$). Conventional M-QAM is a two-dimensional (2D) signaling scheme which can be
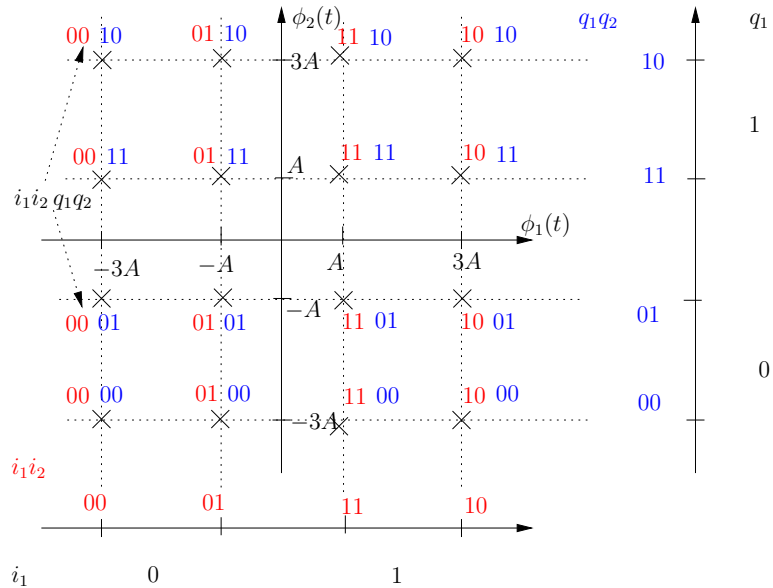
Figure 1.2: Mapping of bits into symbols in 16-ary QAM, in a scatter pattern representation of the constellation.

considered as a concatenation of (i) $\sqrt{M}$ pulse amplitude modulation (PAM) along the in-phase (I) signaling dimension, and (ii) $\sqrt{M}$ PAM along the quadrature (Q) signaling dimension [7]. QAM operates by transmitting two DSB signals via a carrier
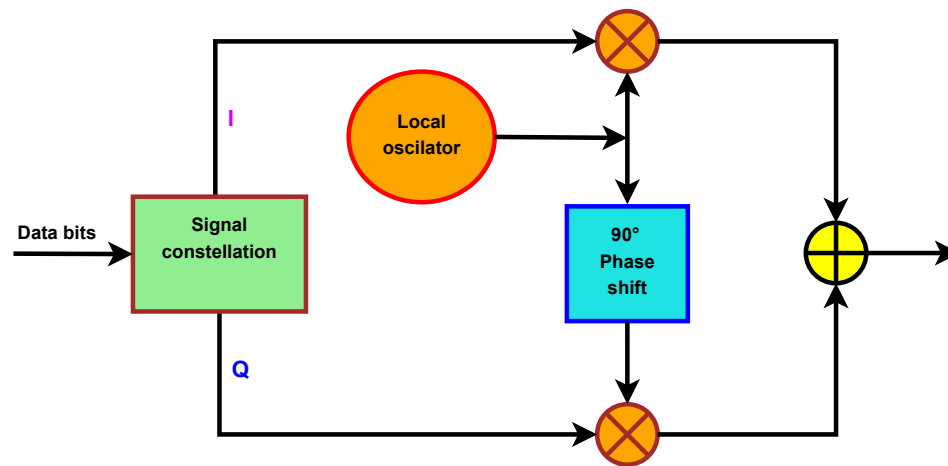
Figure 1.3: QAM modulator.

of the same frequency, but in phase quadratures, as shown in Figure 1.3. In QAM, as the modulation level increases, the number of bits per symbol increases, which improves the bandwidth efficiency as measured in terms of [bps/Hz]. However, for received signals with a given average power, the signal points are brought into closer proximity, which increases the susceptibility to noise and interference.

Spatial Shift Keying

Spatial shift keying modulation is a recently developed transmission technique that uses multiple antennas to encode information in the spatial index of the specific antenna activated in the array, for transmission of the unmodulated carrier [33]. SSK successfully exploits the indices of the transmit antennas as a signaling dimension for sending spatial symbols [34]. Activating one transmit antenna at a time eliminates channel interference and antenna synchronization, and also creates a robust system for channel estimation errors, since the probability of error is determined by the channel characteristics associated with the physical location of antennas, rather than the channel realization [35] [36].

Spatial Modulation

The process of combining two (or more) information bearing signals into a single RF carrier is referred to as concatenated (hybrid) modulation. Spatial modulation is a concatenated modulation which combines SSK modulation with conventional amplitude phase modulation (APM) [37]. SM can be interpreted as a 3D signaling scheme where the I and Q components represent the first two dimensions, and antenna selection represents the third dimension [38] as shown in Figure 1.4.
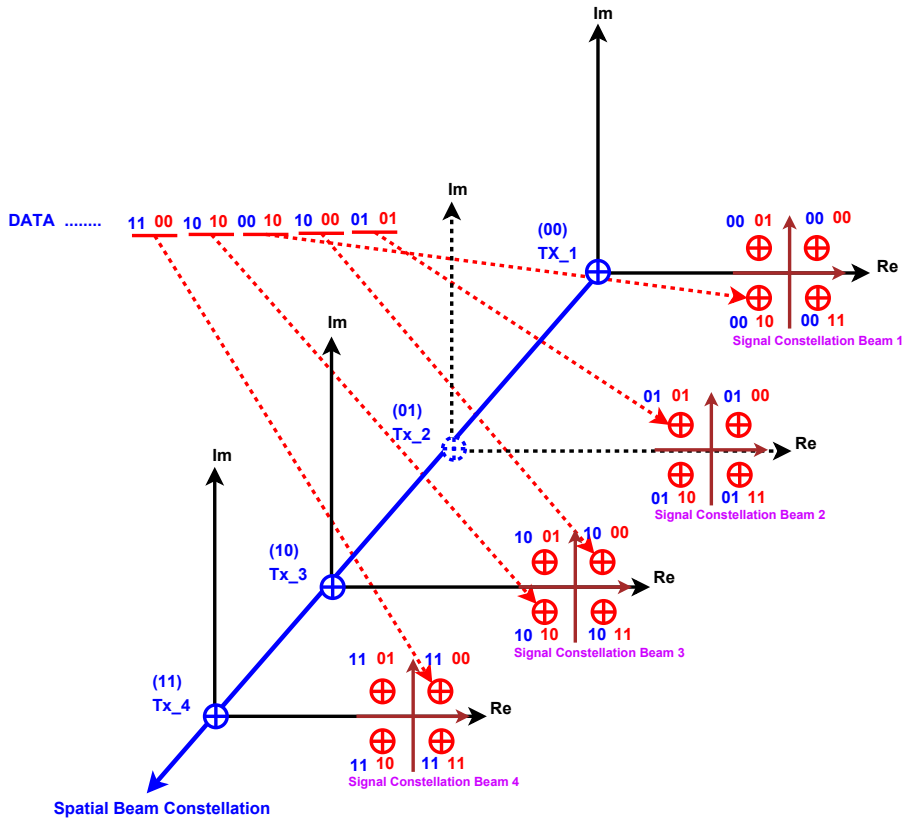
Figure 1.4: Illustration of the 3D encoding of spatial modulation.

The benefit of this scheme is that it requires only a subset of RF chains (as few as one), in contrast to conventional MIMO systems [39] [40]. The use of the transmit antenna number as an information bearing unit increases the overall spectral efficiency

by the base two logarithm of the number of transmit antennas.

1.2.2 Bandwidth Efficiency

In general, in communication systems, spectral efficiency refers to the data rate that can be accommodated in a given bandwidth to achieve acceptable performance (i.e., reasonable fidelity). Spectral efficiency is measured in bits per second per hertz (bits/s/Hz) and is defined as:

$$\eta_s = \frac{R_b}{B_w}(\text{bit/s/Hz})$$

where R is the data rate in bit/s, and B_w is the passband transmission bandwidth in Hz.

An M-ary QAM is based on M alternative symbols, with $k = \log_2(M)$ bits/symbol. Since QAM is a form of double sideband passband transmission, the spectral efficiency cannot exceed k (bit/s)/Hz. The upper bound bit rate (capacity) for M-ary QAM in a noise-free channel with rectangular pulse shaping at the baseband is given by the formula:

$$C = 2 \cdot B_w \cdot \log_2(M)$$

Basically, there are two ways to increase the speed of data transmission: by using more bandwidth, and by using more signal levels [41].

Through an N_t element transmit antenna array, SM merges a spatial dimension with conventional QAM modulation without any bandwidth expansion, and increases the system bandwidth efficiency by $\log_2 N_t$ in comparison to SISO QAM.

1.2.3 Wireless Communication Channels

The performance of wireless communication systems is affected by the wireless channel propagation environment. Here the term channel describes the impulse response of the linear time-varying communication system between a transmitter and a

receiver. Sound modeling of wireless channels plays an essential role in analyzing and designing wireless transceivers. In essence, transmitted signals are subject to detrimental effects such as signal attenuation (deterministic power loss with distance), fading and shadowing (multiplicative random effects) as well as the omnipresent additive white Gaussian noise (AWGN) in the receivers. This section reviews some of the wireless communication channel theory relevant to this dissertation.

Generally, in addition to deterministic path losses, wireless links are impaired by random fluctuations of the signal level in the time, frequency and/or space domains. This channel behavior is known as fading and impacts the performance of the wireless system, depending on the fading model. The most common type of fading is flat, slow fading where the multiplicative factor affecting the signal received at the baseband is given by a complex random variable denoted as h. In the most common (and worst) case Rayleigh fading statistical model, h has real and imaginary Gaussian components with zero means, which are independent and identically distributed (i.i.d.) RVs [42].

Even though fading adversely affects system performance in most communication systems, some signaling techniques use the fading environment as an opportunity to enhance system performance. For example, MIMO systems in multiplexing configurations create multiple parallel data links to improve the bandwidth efficiency.

1.2.4   Signal Propagation

In a wireless communication channel, a transmitted signal can reach the receiver through line-of-sight (LOS) as well as non-line-of-sight (NLOS) paths. The main NLOS propagation mechanisms are reflection, scattering, and diffraction. There are also other mechanisms of propagation, such as tropospheric or ionospheric scattering, but these are not common in most wireless communication systems. An important component of this work is signal propagation in the channel. In particular, small-scale propagation phenomena are important, because they influence physical layer

and modulation scheme designs [43].

In this dissertation, it is assumed that the communication channel is a rich reflective environment with a number of different LOS and NLOS paths between the transmitter and receiver that can be selected via different angles of signal departure from the transmitting antenna array. With this provision, the electromagnetic field at the receive antenna is the sum of the free space field from the transmit antenna plus the reflected and scattered free space waves from each of the reflecting and scattering obstacles in the channel environment. This is an acceptable assumption for most indoor and outdoor communication channels. If this condition is not satisfied, the system designer should include reflectors in the communication link design. Such reflectors or RF mirrors are already used in many microwave RF links.

1.2.5   MIMO Systems

Wireless communication system designers are facing a variety of challenges. These including radio frequency spectral scarcity and a complex space-time varying wireless channel. In addition, there is an increasing demand for higher throughput, higher quality of service, and higher system capacity. Recently, MIMO systems have emerged as a promising technology capable of satisfying these demands. MIMO communication systems can be defined intuitively by considering that multiple antennas are used at the transmitter and receiver ends. The key idea behind MIMO is that signals sampled in the spatial domain at both ends are combined to create effective multiple parallel spatial data channels (to increase the data rate), and/or to add diversity to improve the reliability (reduce the BER) of the communication system [44].

The advantages of deploying multiple antennas result from utilizing a new dimension, space, in addition to the dimensions of time and frequency. Hence, because the spatial dimension complements the time dimension, MIMO technology is also known as a space-time wireless system. Until the mid-1990s, antenna arrays were primarily

used at the receiver for estimating the direction of arrival, contributing to beam-forming and spatial diversity. With the emergence in 1995 of what is now known as conventional MIMO systems, multipath signals were exploited to benefit multi-plexing and/or diversity gain. In MIMO systems, since space is used as an additional dimension, it needs to be modeled separately, similarly to the way time and frequency variations have been modeled for wideband SISO systems.

1.2.6   Diversity

To combat the impact of fading on the bit error rate (BER), diversity techniques are usually employed. The underlying principle of diversity techniques is to provide the receiver with multiple versions of the same transmitted signal. Each of these versions is defined as a diversity branch. If these versions are affected by independent fading conditions, the probability that all branches fade at the same time is dramati-cally reduced. Hence, diversity helps to stabilize the link through channel hardening, which leads to improved performance in terms of BER. Because fading may take place in time, frequency or space, diversity techniques may be exploited similarly in each of these domains.

The concept underlying spatial diversity techniques is that, in the presence of ran-dom fading caused by multipath propagation, the SNR can be significantly improved by combining the output of decorrelated antenna elements.

Diversity techniques used to mitigate degradation in error performance due to wireless fading channels include:

- Spatial diversity: multiple antennas that are sufficiently separated (by more than 10λ) are used to implement independent wireless channels, where λ is the carrier wavelength dependent on the carrier frequency.

- Polarization diversity: independent channels are implemented by using the fact

that vertically and horizontally polarized paths are independent.

- Time diversity: the same information is transmitted repeatedly at time instances that are sufficiently separated (by more than the coherence time).

- Frequency diversity: the same information is transmitted repeatedly at frequency bands that are sufficiently separated (by more than the coherence bandwidth).

- Angle diversity: multiple receive antennas with different directivity are used to receive the same information bearing signal at different angles.

In the case of frequency/time diversity, the same data are transmitted at multiple spectral bands/times to achieve diversity gain. Time diversity and frequency diversity techniques require additional time and frequency resources, respectively. However, antenna and spatial diversity techniques do not require any additional time or frequency resources. Space-time diversity techniques are illustrated in Figure 1.5. In the case of space-time diversity, data is transmitted over multiple "paths" in the same time slots.
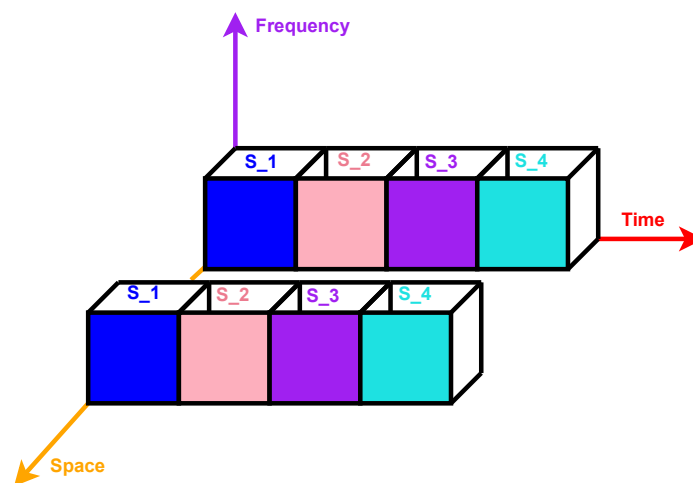
Figure 1.5: Space-time diversity techniques.

Since channel capacity and diversity gain decrease as the correlation between the antenna elements increases, antenna spacing must be large enough to reduce the signal correlation at different antennas.

1.2.7 Space-Time Block Coding

Space-time block codes (STBCs) have evolved considerably over the years. While they originally attracted attention due to their low decoding complexity, they have been subject to renewed interest in light of the diversity-multiplexing trade-off. Theoretically, STBCs may take several forms, but practically, linear STBCs are by far the most widely used. The idea behind linear STBCs is to spread information symbols in space and time, to improve either the diversity gain or the spatial multiplexing rate, or both.

Orthogonal space-time block codes (O-STBCs) are a very important subclass of linear STBCs in conventional MIMO systems. They have properties which make them extremely easy to decode, while still achieving a full diversity of $N_t \times N_r$, where N_t and N_r represent the number of transmit and receive antennas, respectively. In fact, in the case of O-STBCs, MIMO maximum likelihood decoding decouples into several SIMO maximum likelihood decodings. Each transmitted symbol is thus decoded independently of the other symbols transmitted within the same block. However, O-STBCs have a much lower spatial multiplexing rate than is the case with spatial multiplexing schemes [45].

The best-known O-STBC is the Alamouti code. It is a complex O-STBC for two transmit antennas and is characterized by a multiplexing rate of 1. Beamforming techniques all require knowledge of the channel at the transmitter to derive optimal weights. In contrast, Alamouti developed an ingenious but straightforward transmit diversity scheme for two transmit antennas, known as the Alamouti scheme, which

does not require the channel gain to be known at the transmitter. In the Alamouti scheme, two symbols S_1 and S_2 are transmitted simultaneously from the first and second antennas during the first symbol period, followed by the transmission of symbols $-S_2^*$ and S_1^* from the first and second antennas during the next symbol period [46]. The linear decoding technique with two receive antennas, for this 2×2 MIMO configuration, has a low complexity and achieves the maximum diversity gain of 4.

Alamouti further developed the scheme to work with two transmit antennas and M_R receive antennas, with a diversity order of $2M_R$. Because of its simplicity, the Alamouti scheme is a popular candidate for improving the reliability of new MIMO systems and is pursued later in this dissertation.

1.2.8 Multiple Access with SDMA

One of the most important emerging problems for communication system designers is the application of MIMO concepts to multiuser environments. Traditional multiuser communication systems use one or more of the time, frequency and code division multiple access approaches to share a limited frequency spectrum. The best multiplexing scheme for a given application is dependent on the characteristics of the particular channel of interest. The use of antenna arrays in a multiuser channel permits a further type of multiplexing, often referred to as spatial multiplexing. Spatial multiplexing is particularly attractive because it can easily be used in conjunction with other forms of multiplexing to dramatically improve the number of users that can share a given channel. In addition to promising improved capacity for future communication networks, in some cases these methods can be applied to existing communication protocols, thus extending their usefulness. Below is a brief description of some multiple access techniques.

FDMA (frequency division multiple access)

FDMA is the most popular method of multiple access and was the first technique to be employed in modern wireless applications. In FDMA, the available bandwidth is split into a number of equal bandwidth sub-bands, each of which is assigned to a unique user.

TDMA (time division multiple access)

TDMA is another widely known multiple access technique and succeeded FDMA in modern wireless applications. In TDMA, the entire bandwidth is made available to all users but on a time-sharing basis.

CDMA (code division multiple access)

CDMA is a nonconventional multiple access technique, in which the entire bandwidth is made available simultaneously to all users. In CDMA, signals are differentiated by means of code sequences or signature sequences which correspond to different users. Each transmitter-receiver pair is allocated one code sequence, with which communication is established. At the reception side, detection is carried out by means of a correlation operation.

SDMA (space division multiple access)

SDMA is a multiple access technique that creates parallel spatial pipes for simultaneously transmitting user signals by differentiating among user locations. SDMA is implemented in modern wireless systems primarily in combination with other multiple access techniques. In SDMA, the entire bandwidth is made available simultaneously to all user signals and signals are differentiated spatially.

1.3 Antenna Arrays

Antenna arrays are becoming increasingly important in wireless communications because they have many advantages, including:

- Beamforming functionality (radiation pattern direction in space)

- Higher gain (directivity) in comparison to a single-antenna system

- Diversity gain in multipath channels

- Array signal processing

An important characteristic of an antenna array is that the radiation pattern can be changed in response to different excitations of the antenna elements. Unlike the fixed radiation pattern of a single antenna, an antenna array radiation pattern, referred to as an array pattern, can be changed by exciting the antenna elements with different currents (magnitudes and phases). This provides another degree of freedom in choosing a desired array pattern from an array, without changing its physical dimensions or position [47]. Furthermore, by manipulating the signals received by the individual antenna elements in different ways, it is possible to achieve many signal processing functions such as direction-of-arrival (DOA) estimation, spatial filtering, interference suppression, gain enhancement, and target tracking. According to the reciprocity theorem, the radiation patterns of an antenna in the transmitting mode is the same as the those for the antenna in the receiving mode. A diagram classifying antenna array applications is provided in Figure 1.6.

1.3.1 Smart Antennas

A smart antenna refers to an antenna array that is controlled by an advanced signal processing system that can adjust or modify the antenna array radiation pattern in
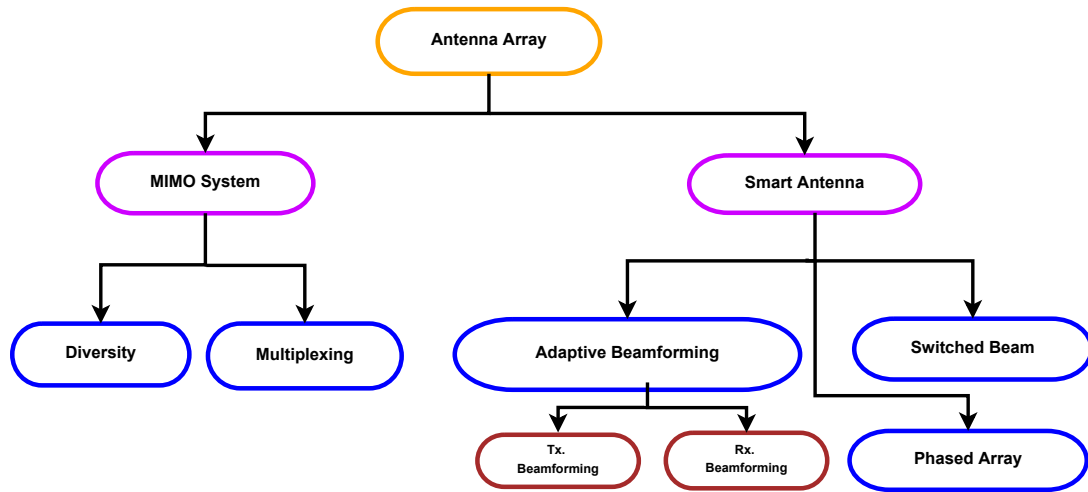
Figure 1.6: Antenna array applications.

order to maximize signals of interest and minimize interfering signals [48]. In general, smart antennas include both switched beam and beamformed adaptive systems [49]. Specifically, switched beam systems contain a distinct number of available fixed radiation beam patterns. Based on the system requirements, a control unit selects which beam to access at any given time. In contrast, adaptive beamforming systems allow the antenna array to steer the beam in any desired direction while at the same time nulling interfering signals. The smart antenna concept implies the ability of the system to implement judicious control of the desired direction of the transmitted radiation pattern. This contrasts with a fixed beam ("not smart") antenna, which lacks the ability to modify the radiation pattern according to the variable channel environment. The "smart technology" terminology is used to identify more accurately an adaptive array that has advanced control and monitoring subsystems, Figure 1.7. In summary, some of the numerous benefits of smart antennas are:

- System capacity improvements

- Greater admissible signal bandwidths
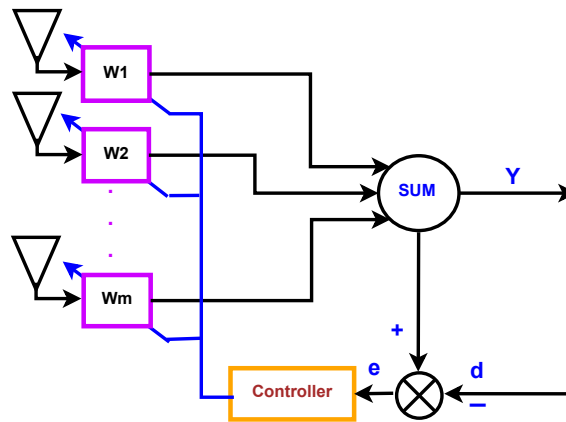
Figure 1.7: Smart antenna processing.

- Space division multiple access (SDMA)

- Higher signal-to-interference ratios

- Null steering

- Reduction of multipath effects

- Enhanced AOA estimation and direction finding accuracy

- Improved array resolution

1.3.2   Uniform Linear Arrays

Smart antennas are composed of a group of two or more antennas working to-gether to build a special radiation pattern in the propagation channel. The most straightforward array geometry is the linear array, where all elements are aligned in a straight line and generally have uniform inter-element spacing. Linear arrays are the fundamental array to analyze, and many valuable insights can be obtained by understanding their behavior. The most basic array which can be considered is the two-element array. A two-element array demonstrates the same general behavior as

much larger arrays and provides a good starting point for understanding the phase relevance between array elements [50].

Figure 1.8 shows two vertically polarized infinitesimal dipoles aligned along the y-axis and separated by a distance d. The field point is located at a distance r from the origin such that $r >> d$. It can therefore be assumed that the distance vectors $\bar{r}_1, \bar{r}$ and $\bar{r}_2$ are all approximately parallel to one another.
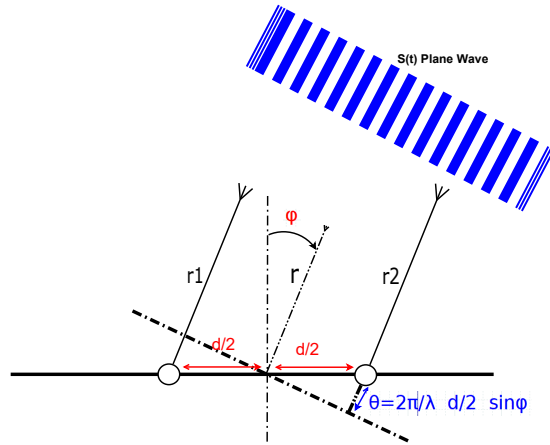
Figure 1.8: Uniform linear antenna array.

For a single plane wave $S(t)$ arriving from the direction of φ, the delay θ, between received signals at two adjacent elements of the array referenced to the array center point, can be expressed as follows:

$$\theta = \frac{2\pi}{\lambda} \frac{d}{2} \sin \varphi \tag{1.1}$$

One method of creating fixed beams is through the use of Butler matrices. A Butler matrix provides an analog means of producing several simultaneous fixed beams by using phase shifters.

Throughout the dissertation, most of the time, we assumed that the spacing between antenna elements (d) in the receiver during the operation phase is the same as the carrier wavelength $(d = \lambda)$. However, it is understood that for proper AOA estimation during the training phase distance between the element should be half of the

wavelength. $(d = \frac{\lambda}{2})$.

1.3.3 Beamforming

Almost every antenna, depending on its E and H field components, has a distinctive radiation pattern. These patterns typically indicate the antenna radiating power intensity as a function of azimuth (horizontal plane) and elevation (vertical plane) angles, respectively [48].

Beamforming is a powerful technique [51] [52] which increases the RF link signal-to-noise ratio (SNR) by focusing energy in the direction of the target (desired receiver). In an antenna array, by adjusting the current phase and amplitude feeding each element of the array, the main lobe of the antenna array pattern can be directed at a desired angle; this process is referred to as beamforming. Beamforming intensifies the strength of the desired signal at the receiver. When receiving, the antenna array can null or suppress interference from undesired signals arriving from angles that do not match the AOA from the desired transmitter. Moreover, beamforming is also used for many other purposes, including:

- Overcoming signal propagation issues, such as greater path losses at millimeter wave frequencies

- Providing the ability to shape and steer beams dynamically to specific users (spatial filtering)

- Improving the performance of a communication system for a target user

- Increasing the capacity and coverage of a communication system

Conventional transmit beamforming provides the simplest approach for increasing system capacity and coverage in the downlink.

Before discussing true beamformers, it is worth mentioning that an initial, simple solution for the downlink is to implement a switching technique between fixed beams. Multiple non-overlapping beams are formed to cover a given angular sector. First, a sounding procedure determines the strongest uplink signal for each of the beams. In the downlink, the same beam is then used for transmission. If the chosen beam remains the best beam for a sufficiently long period of time, the control algorithm can be very simple. However, this technique assumes that the uplinks and downlinks are reciprocal.

A null-steering beamformer technique can produce nulls in as many as $n_t - 1$ directions. Thus, it can cancel interfering signals in the direction of $N_r \leq N_t - 1$ users. Fixed beamforming can relax frequency limitations in the downlink, because the same frequency can be reused within the same cell due to spatial filtering. It is also possible to use different frequencies for different beams.

1.3.4 Direction of Arrival

A radiated signal departs from the transmitter in a particular direction (φ_t) and arrives at the receiver from a specific direction (φ_r). Thus, the channel also depends on φ_t and φ_r. This can be interpreted as a directional distribution of the energy at both sides of the link.

Angle-of-arrival (AOA) estimation has also been referred to as spectral estimation and direction-of-arrival (DOA) estimation. Figure 1.9 shows M incident complex signals arriving from M directions. They are received by an array of N_r elements with N_r possible weights. Each received signal $X(k)$ includes additive Gaussian noise with a zero mean. Time is shown by the kth time sample. Thus, the array output $\mathbf{y}$ can be specified in the following form:
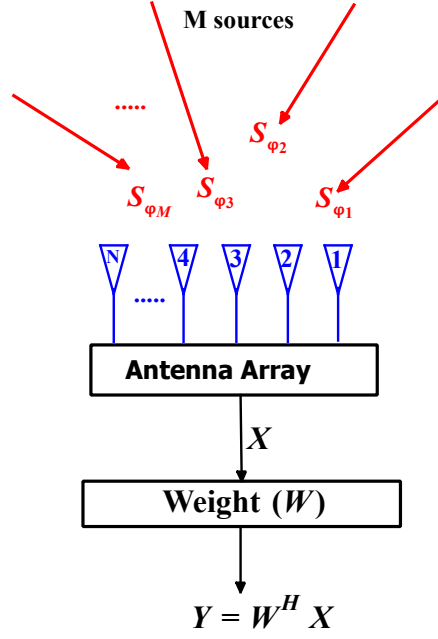
Figure 1.9: Receiver antenna array.

$$\mathbf{Y} = \mathbf{W}^T \mathbf{X} \tag{1.2}$$

$$\mathbf{X} = \mathbf{D} \cdot \mathbf{S} + \mathbf{n} \tag{1.3}$$

$$\mathbf{D} = [\mathbf{d}(\varphi_1)\, \mathbf{d}(\varphi_2)\, \ldots\, \mathbf{d}(\varphi_M)] \tag{1.4}$$

where $\mathbf{D}$ is referred to as the steering matrix, $\mathbf{d}(\varphi_i)$ is the steering vector for the plane wave received at direction φ_i and $\mathbf{S}$ is the vector of plane waves. Many AOA algorithms use this matrix in the estimation process.

Communication schemes developed in this dissertation will proceeds in two stages: (i) the training phase and (ii) the operational phase. In this dissertation, the main contributions are focused on detecting the AOAs. In order to perform ML detection for AOAs in the operational phase of the proposed algorithm, we are going to work with matched filter implementation of ML detection. However, in order to perform

detection for the AOAs, in the training phase of our algorithm, we require to esti-
mate the AOAs that result in optimum SER performance of the proposed detection
algorithm. Even though the AOAs estimation is not deployed directly in this work
because our focus is on designing the operation phase, below we review some possible
techniques that could be used for AOA estimation during the training phase.

There are a variety of algorithms for estimating the AOA, each with different advan-
tages and limitations. Two widely used methods are reviewed in this section, following
the approach developed in [53].

Capon AOA Estimation

Capon AOA estimation is a maximum likelihood (ML) estimation of arriving
power also is known as minimum variance distortionless response (MVDR). This
method estimates the power arriving from the desired direction, while all other sources
are considered as interference. The goal is to maximize the signal to interference ratio
(SIR). Figure 1.10 plots the pseudospectral function for this method. A maximum
likelihood estimate is adopted for a four-element antenna array, assuming two incident
waves with arrival angles given by $\varphi_1 = 20°, \varphi_2 = -5°$. It can be seen that the
pseudospectral function has clear peaks at the angles of arrival of incident waves. In
the case of two or more signals arriving at the receiver, the signal correlation affects
the function resolution. The ML method has acceptable performance in Rayleigh
distributed multipath channels and does not require a priori knowledge of the channel.

MUSIC Algorithm

The multiple signal classification (MUSIC) direction of arrival estimation method
assumes that noise is uncorrelated, which results in a diagonal correlation matrix. It
also assumes that signals are either uncorrelated or mildly correlated. The MUSIC
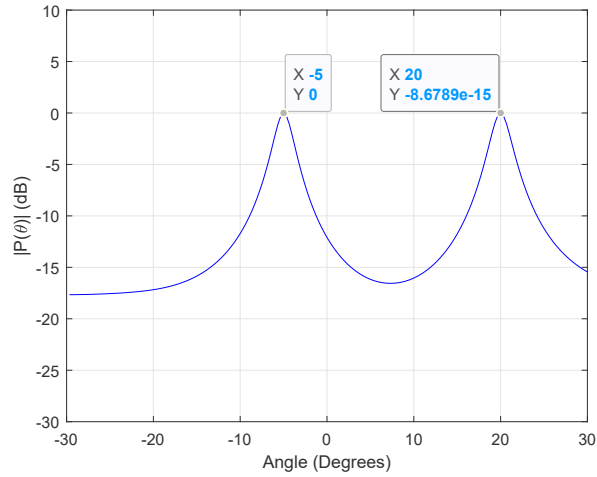
Figure 1.10: pseudospectral function plot with maximum likelihood estimation, for $\varphi_1 = 20°$, and $\varphi_2 = -5°$.

algorithm can precisely calculate the angles of arrival and, consequently, the number of signals as well as the signal power. The plot of the pseudospectral function for MUSIC algorithm is shown in Figure 1.11. The MUSIC estimate algorithm is used for a four element antenna array, two incident waves with arrival angles given by $\varphi_1 = 10°$ and $\varphi_2 = -15°$. The MUSIC pseudospectral function peaks are not an indication of signal power; these peaks represent the roots of the polynomial in the denominator of pseudospectral function. It is clear that MUSIC detection has better resolution than is the case with ML.
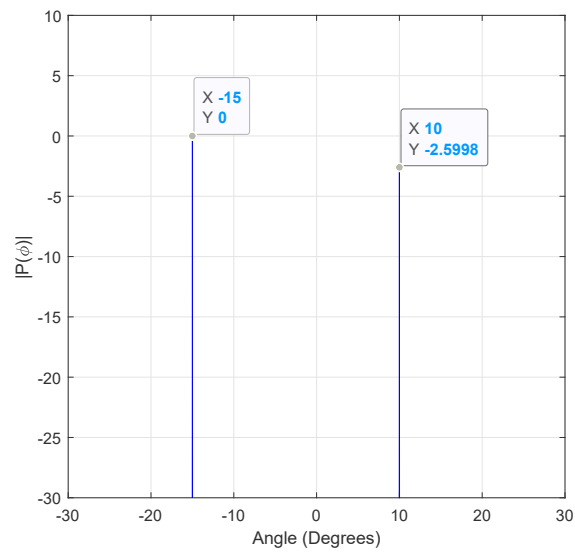
Figure 1.11: Pseudospectrum function plot with MUSIC estimation, for $\varphi_1 = 10°$ and $\varphi_2 = -15°$.

2 Antenna Transmitting Pattern Beam Angle Shift Keying Modulation

This chapter introduces beam angle shift keying (BASK) modulation, which uses an antenna array to encode information symbols in the angle of RF wave propagation departure and arrival in a MIMO wireless channel, as shown in Figure 2.1. Specifically, at the transmitter, a block of information bits is mapped into a "spatial" symbol selecting the beam, or equivalently the direction of departure, for the unmodulated carrier signal. Via specular reflection paths, the carrier signal is assumed to arrive at the receiver from one direction for the duration of the spatial symbol indexing the transmitter/receiver antenna array beam. By using receiver antenna array signals, an ML detection is derived to differentiate between the AOAs of different beams.

This chapter is organized into six sections. The first section introduces the system model as well as transmission and reception methodology. Section 2.2 presents the proposed modulation scheme. Section 2.3 describes the demodulation process. Section 2.4 examines the detection algorithm and symbol error rate in more detail. The performance analysis and simulation results are presented in Section 2.5. Finally, Section 2.6 summarizes the chapter.
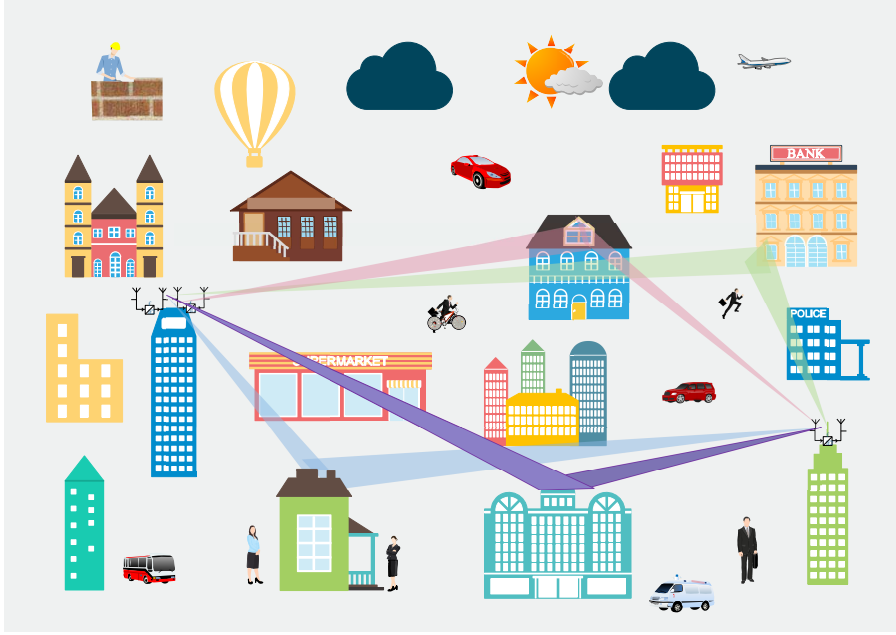
Figure 2.1: MIMO channel environment.

2.1 Antenna Beam Switching Communication System

In this section, the BASK system model is explained by presenting the operational principles of the transmitter and receiver, as shown in Figures 2.3 and 2.4, respectively.

In this system, the transmitted signal is a continuous wave (CW), i.e., a carrier signal that does not carry information at the baseband as in conventional transmission techniques. In the proposed system, the data/spatial symbols S_i are encoded in the index i ($i \in \{1, 2, \cdots, M\}$) of the beam angle for the signal transmitted from the antenna array, and the number of beams represents the modulation level M, Figure 2.2. Assuming a non-line-of-sight (NLOS) channel for the specific transmitted beam with an angle θ_i through a single (dominant) reflection, the plane wave signal at the receiver arrives at the corresponding AOA φ_i. The AOA induces on the receive antenna array the spatial signature that is used to resolve the spatial symbols
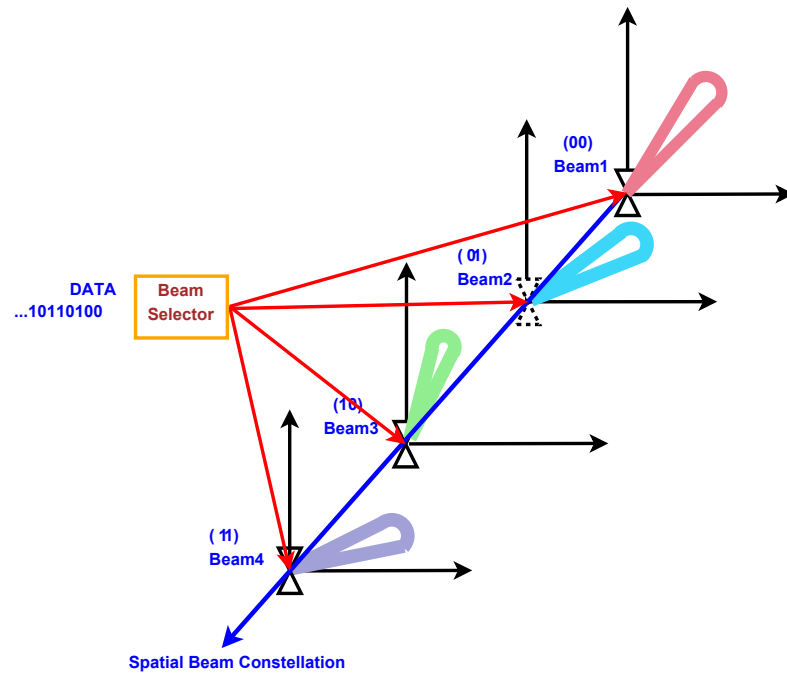
Figure 2.2: Illustration of 1D data encoding in the BASK modulation.
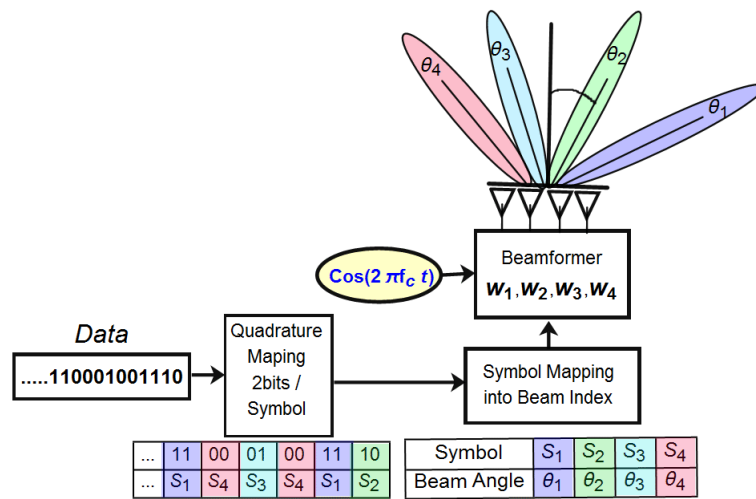
Figure 2.3: BASK transmitter.

represented by the index i in the angular domain [6]. In BASK, the modulation level

M depends on the number of resolvable beam angles at the receiver, for the targeted symbol error rate (SER). The resolvable beam angles are a group of M beam angles which the distances between the associated spatial symbols result in an SER comparable to SER for the same level classical modulation. The spatial symbols S_i represent $\log_2(M)$ data bits. The one-to-one mapping between S_i and the angle of departure (AOD) - θ_i -, AOA - φ_i - is shown in Table 2.1.

Table 2.1: Mapping between spatial symbols and departure and arrival beam angles.

Symbol	S_1	S_2	...	S_M
Angle Of Departure	θ_1	θ_2	...	θ_M
Angle Of Arrival	φ_1	φ_2	...	φ_M

Traditionally, when the transmitter antenna array focuses its signal in an optimized direction, θ, the antenna gain serves to improve the signal-to-noise ratio (SNR) at the receiver, in comparison to what can be achieved with omni-directional antennas. In the proposed system, the transmit beam directions θ_i offer antenna as well as multiplexing gain. When beamforming with the antenna array, the system transmits a carrier signal in direction θ_i by applying a weighting vector $\mathbf{W}_i$ to the signal feeding antenna elements in the transmitting antenna array. The magnitude of $\mathbf{W}_i$ is the same as the number of elements in the antenna array. A larger number of elements ensures that the synthesized far-field patterns more effectively confine energy radiation to the desired directions. This provides improved selectivity for differentiating among the received beams [47].

For each symbol, S_i, the transmitter assigns not only a unique AOD θ_i but also $\mathbf{W}_i$. The transmitter switches between the M beams according to the symbols transmitted by using only one beam (out of M possible beams). The beam switching rate R_{BASK} is equal to the system symbol rate R_s. More details concerning the phased array design and operation lie outside the scope of this work. It is further assumed that the
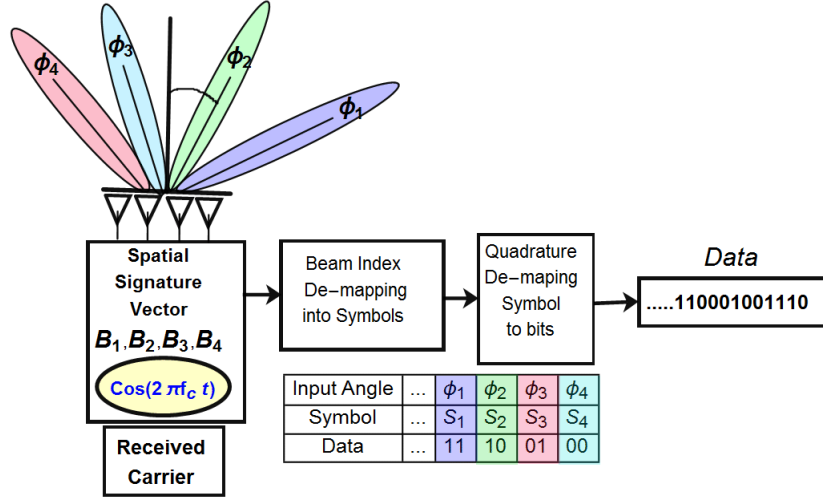
Figure 2.4: BASK receiver.

signals arriving at the receiver antenna array are in the far-field of the beamforming array. This ensures that the radiation impinging on the receiving antenna array is in the form of a sum of plane waves.

Communication in the proposed system proceeds in two stages: (i) training, and (ii) maximum likelihood detection. In the first stage, the transmitter trains the receiver for the AOAs associated with all spatial symbols. During the training phase, in a practical implementation, the transmitter may send signals in more than M different directions, so that by estimating AOAs the receiver can decide on the M spatial signatures offering the best signal discrimination (with the lowest SER).

In the second stage, assuming the angular characteristics of the channel have not changed from the training phase, the receiver uses maximum likelihood (ML) detection or corresponding maximum correlation algorithms to detect the AOA among the M possible choices determined in the training phase.

For the remainder of this chapter, without loss of generality, unless stated otherwise it will be assumed that $M = 4$, i.e., the system has four beams and each symbol carries 2 bits/symbol.

2.2   BASK Transmitter

In the transmitter, the RF carrier is fed to the beamformer unit and is transmitted continuously from the antenna array, as shown in Figure 2.3. Assuming that $M = 4$, the modulator maps the two incoming bits into the designated 1D spatial symbols (S_1, S_2, S_3, S_4). The beam index mapping block correlates the symbols with unique beam angles of departure, θ_i, and corresponding weighting vectors, $\mathbf{W}_i$, as presented in Table 2.2.

Table 2.2: Symbol Mapping to Antenna Beam Angles and Weighting Vectors.

Symbol	S_1	S_2	S_3	S_4
Angle Of Departure	θ_1	θ_2	θ_3	θ_4
Weighting Vector	$\mathbf{W}_1$	$\mathbf{W}_2$	$\mathbf{W}_3$	$\mathbf{W}_4$

For a given beam angle/spatial symbol indexed by i, with N_t elements in the transmitting antenna array see Figure (2.3), the radiated signal from the antenna elements in a vector format is:

$$\mathbf{R} = S(t) \cdot \mathbf{W} \tag{2.1}$$

$$\begin{bmatrix} R_1 & R_2 & \cdots & R_{N_t} \end{bmatrix} = S(t) \cdot \begin{bmatrix} w_i^1 & w_i^2 & \cdots & w_i^{N_t} \end{bmatrix} \tag{2.2}$$

where $S(t)$ is the CW and w_i^n are the complex coordinates of $\mathbf{W}_i$ ($n \in \{1, \cdots, N_t\}$). For a uniform linear array (ULA) with antenna elements separated by a distance d, with NLOS communications, to concentrate the energy in θ_i:

$$w_i^n = e^{jn \cdot \alpha_i}$$

where

$$\alpha_i = \frac{2\pi}{\lambda} \frac{d}{2} \sin \theta_i$$

and λ represents the carrier wavelength.

This applies the required relative phase shifts to signals feeding the different antenna array elements to ensure in-phase addition in the desired AOD. For other antenna array configurations, different one-to-one mappings between the weighting vectors and beam angles are used in Table 2.2.Ultimately, it is the AOA rather than the AOD that determines system performance; AOAs depend not only on the radiation patterns but also on the geometry of scatterers in the wireless medium.

2.3   BASK Receiver

During the training phase of the transmission, the receiver receives information about the M possible incoming signal directions, and for every AOA φ_k the receiver knows the corresponding spatial symbol S_k. The BASK receiver uses an efficient AOA estimation algorithm (for instance ML) to decide (for the symbol duration) on the signal AOA φ_k. In this work, it is assumed that the receiver uses a ULA with N_r elements equally spaced at distances of d. A signal received from any direction represents a form of on-off keying for the carrier. With a matched filter at every antenna element, after downconverting, in the absence of noise and taking a sample for every symbol, the received signal vector at the baseband for $M = 4$ is represented as:

$$\mathbf{B}_{\varphi_k} = \sqrt{E_s} \cdot \begin{bmatrix} e^{-j3\frac{2\pi}{\lambda} \cdot \frac{d}{2} \cdot \sin(\varphi_k)} \\ e^{-j\frac{2\pi}{\lambda} \cdot \frac{d}{2} \cdot \sin(\varphi_k)} \\ e^{j\frac{2\pi}{\lambda} \cdot \frac{d}{2} \cdot \sin(\varphi_k)} \\ e^{j3\frac{2\pi}{\lambda} \cdot \frac{d}{2} \cdot \sin(\varphi_k)} \end{bmatrix} \tag{2.3}$$

if the signal arrives from the direction φ_k ($k \in \{1, 2, \cdots, M\}$). Considering the same azimuthal plane for the reflected RF signal and the receiving antenna array, the term

$$d_{\pm n} = \pm n \frac{d}{2} \cdot \sin(\varphi_k) \qquad n = \begin{cases} \{1, 3, 5, \cdots, \frac{N_r}{2} + 1\} & n\ even \\ \{0, 2, 4, \cdots, \frac{N_r + 1}{2}\} & n\ odd \end{cases}$$

represents the difference in distance traveled by the plane wave to various receiving antenna array elements relative to center of the array, as shown in Figure 2.5.
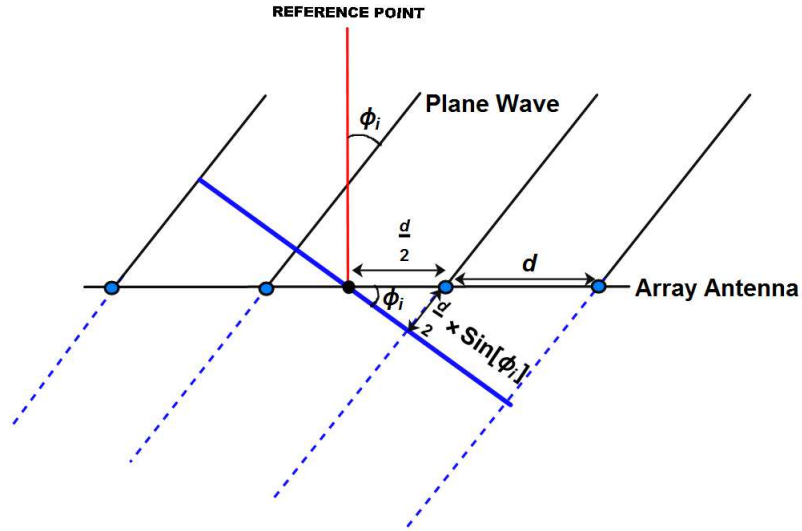
Figure 2.5: Relative phase shifts in a uniform linear array (ULA).

In this dissertation, it is assumed that the signals arriving from different directions have the same energy E_s at every receiver antenna element. If this is not the case, as determined during the training phase, then the weighting vectors $\mathbf{W}_i$ at the transmitter in Table 2.2 have to be adjusted for magnitude as well as phase. Different path lengths introduce different delays and different phase shifts of the carrier signal received at different elements of the antenna. By defining the base phase shift for direction k as

$$\beta_k = \frac{2\pi}{\lambda} \frac{d}{2} \sin(\varphi_k)$$

then (2.3) can be represented by:

$$\mathbf{B}_{\beta_k} = \sqrt{E_s} \cdot \begin{bmatrix} e^{-j3\beta_k} \\ e^{-j\beta_k} \\ e^{j\beta_k} \\ e^{j3\beta_k} \end{bmatrix} \tag{2.4}$$

Both representations, $\mathbf{B}_{\beta_k}$ and $\mathbf{B}_{\varphi_k}$, define the spatial signatures induced on the receiver antenna array by the transmitted signal, which are used to determine AOAs, or equivalently the spatial symbols, as shown in Table 2.3.

Based on M possible spatial signatures, as in (2.3) or (2.4), in an additive white Gaussian noise (AWGN) channel, the optimal ML receiver projects the received signal vector onto the spatial signatures, as discussed in the next section.

Table 2.3: Mapping between spatial symbols, AOAs, and spatial signature vectors.

Symbol	S_1	S_2	S_3	S_4
Angle Of Arrival	φ_1	φ_2	φ_3	φ_4
Spatial Signatures	$\mathbf{B}_{\varphi_1}$	$\mathbf{B}_{\varphi_2}$	$\mathbf{B}_{\varphi_3}$	$\mathbf{B}_{\varphi_4}$

2.4   BASK Detection Algorithm

There are several possible methods for estimating and detecting AOAs. Depending on the channel and interference models, implementation complexity, etc., these methods result in different performance [54]. In the presence of AWGN alone, with equiprobable symbols, the optimum receiver is a maximum likelihood (ML) receiver which chooses the receive symbol index that offers the smallest Euclidian distance between the received signal and all possible spatial signature vectors. Specifically, assuming that the signal arrives from φ_k, after downconverting, the received vector

signal of size $N_r \times 1$ is:

$$\mathbf{S} = \mathbf{B}_{\beta_k} + \mathbf{N} \tag{2.5}$$

where $\mathbf{N} = [n_1, \cdots, n_{N_r}]^T$, $\mathbf{S} = [s_1, \cdots, s_{N_r}]^T$ and T stands for transpose. The complex RV n_i represents scalar AWGN at the i-th antenna ($n_i \sim \mathcal{CN}(0, \sigma^2)$), and n_i's are independent and identically distributed (i.i.d.). Following standard derivations, the log-likelihood ratios are:

$$L_k = ||\mathbf{S} - \mathbf{B}_{\beta_k}||^2 = \sum_{i=1}^{N_r} \left| s_i - \mathbf{B}_{\beta_k}(i) \right|^2 \tag{2.6}$$

$$= \sum_{i=1}^{N_r} |s_i|^2 + \sum_{i=1}^{N_r} |\mathbf{B}_{\beta_k}(i)|^2 - 2 \cdot \Re\left(\sum_{i=1}^{N_r} s_i \cdot \mathbf{B}_{\beta_k}(i)^* \right) \tag{2.7}$$

where $||\cdot||$ is the L_2 norm of a vector, $\Re(\cdot)$ and * represent the real part and complex conjugate, respectively, and $\mathbf{B}_{\beta_k}(i)$ is the ith coordinate of $\mathbf{B}_{\beta_k}$ as given in (2.4). Assuming the same energy for all received spatial signature vectors ($N_r \cdot E_s$), the ML receiver is the maximum correlator receiver which projects the received signal $\mathbf{S}$ onto all possible spatial signature vectors, $\mathbf{B}_{\beta_k}$ ($k \in \{1, \cdots, N_r\}$, and decides on the index resulting in the maximum correlation.

2.4.1 Symbol Error Rate in AWGN

For M-ary signaling using ML detection in AWGN channels, the SER can be tightly upper bounded as follows:

$$SER \simeq \frac{M_{min}}{2} \mathrm{erfc}\left(\sqrt{\frac{d_{min}^2}{4N_0}} \right) \tag{2.8}$$

where (i) $\mathrm{erfc}(\cdot)$ is the standard error function complement, (ii) d_{min} is the minimum Euclidian distance between the constellation points (signals in the absence of AWGN) at the receiver, (iii) N_0 is the noise power spectral density (PSD), and (iv) M_{min} is the maximum number of points in the constellation reached with the minimum distance,

from the perspective of any point. For binary signaling, SER is equivalent to BER and $M_{min} = 1$. For a system with M beams/symbols, the number of inter-distances d_{ij} between spatial signature vectors $\mathbf{B}_{\beta_i}$ and $\mathbf{B}_{\beta_j}$ to consider when determining d_{min}^2 is $\binom{M}{2}$, where the binomial coefficient represents the number of two-element subsets from a set with M elements. The inter-distance d_{ij} is calculated as:

$$d_{ij} = \left\| \mathbf{B}_{\beta_i} - \mathbf{B}_{\beta_j} \right\| = \sqrt{E_s} \cdot \begin{bmatrix} e^{-j(2N_r-1)\beta_i} - e^{-j(2N_r-1)\beta_j} \\ \vdots \\ e^{-j3\beta_i} - e^{-j3\beta_j} \\ e^{-j\beta_i} - e^{-j\beta_j} \\ e^{j\beta_i} - e^{j\beta_j} \\ e^{j3\beta_i} - e^{j3\beta_j} \\ \vdots \\ e^{j(2N_r-1)\beta_i} - e^{j(2N_r-1)\beta_j} \end{bmatrix} \tag{2.9}$$

with

$$\beta_i = \frac{2\pi}{\lambda} \cdot \frac{d}{2} \cdot sin(\varphi_i) \tag{2.10}$$

where φ_i is one of M possible AOAs.

For binary signaling with two beams and two receiving antennas ($M = 2$ and $N_r = 2$), (2.9) collapses into:

$$d_{12} = \sqrt{E_s} \sqrt{2 \left((\cos \beta_1 - \cos \beta_2)^2 + (\sin \beta_1 - \sin \beta_2)^2 \right)} \tag{2.11}$$

When $M = 2$ and $N_r = 4$, from (2.9), the distance used in (2.8) is given by:

$$d_{12} = \sqrt{E_s} \sqrt{2 \left((\cos \beta_1 - \cos \beta_2)^2 + ... + (\sin 3\beta_1 - \sin 3\beta_2)^2 \right)} \tag{2.12}$$

In the case of binary signaling, because the single distance d between $\mathbf{B}_{\beta_i}$ and $\mathbf{B}_{\beta_j}$ is a function of two angles, it is relatively easy to find the AOAs φ_1 and φ_2 by using expressions similar to (2.11) and (2.12), resulting in the minimized BER for the arbitrary number N_r of receive antennas.

For a system with $M = 4$,

$$d_{min} = \min \left\{ d_{12}, d_{13}, d_{14}, d_{23}, d_{24}, d_{34} \right\} \tag{2.13}$$

with d_{ij} calculated according to (2.9) and (2.10). In this case, d_{min} is a function of four AOAs: φ_1, φ_2, φ_3 and φ_4. Deciding on the choice of AOAs to maximize d_{min} (or equivalently, to minimize the SER) for a given E_s may require more involved optimization, which is discussed further in the simulation section.

2.4.2   Symbol Error Rate in a Rayleigh Fading Channel

The basis for the proposed system is that the signals at the receiver antenna array arrive along angularly resolvable paths with the same deterministic (average) attenuation, which may be controlled through the magnitude of the weighting vectors $\mathbf{W}_i$. To capture statistical effects for given AOA φ_k, the Rayleigh fading model is assumed for all M angular paths, where the multiplicative scalar channel gains h_k are independent and identically distributed (i.i.d.) complex circular symmetric Gaussian RVs ($h_k \sim \mathcal{CN}(0, 1)$). The signal received in (2.5), in AWGN alone, is now modified to $\mathbf{S} = \mathbf{h}_k \cdot \mathbf{B}_{\beta_k} + \mathbf{N}$. This model assumes one main reflector for a given AOD and corresponding AOA. The multiplicative random gain h_k is the result of smaller scatterers clustered around the main "reflector" for the path determined by AOD and AOA (θ_k and φ_k). Therefore, a plane wave from a given direction, when impinging on the antenna array, undergoes the same fading at all the antenna elements [6]. Because a correlator/linear receiver is used, for slow flat fading channels and coherent detection, with conventional averaging of the SER in AWGN as in (2.8) over the exponentially distributed instantaneous SNR, the upper bound on the SER in the Rayleigh fading channel is as follows [15]:

$$SER \simeq \frac{M_{min}}{2} \left(1 - \sqrt{\frac{\frac{d_{min}^2}{4N_O}}{1 + \frac{d_{min}^2}{4N_O}}} \right) \tag{2.14}$$

where d_{min}^2 is the scaled version of E_s as in the previous subsection, and $\frac{E_s}{N_0}$ represents the averaged SNR (per antenna element) in the Rayleigh fading channel model being considered.

2.5   Simulation Results

In this section, the performance of the BASK modulation with various system parameters and in different channel conditions is evaluated by using Matlab simulations and the results are compared with the analytical results presented in the previous section. Systems are considered with (i) $M = 2$ and $M = 4$ beams/modulation levels, and (ii) $N_r = 2$ and $N_r = 4$ receive antenna elements operating in AWGN and Rayleigh fading channels. This results in eight scenarios, which are summarized in Table 2.4 and referred to subsequently by using NA-MB acronyms.

Table 2.4: System simulation scenarios.

	AWGN		FADING	
	2 BEAMS	4 BEAMS	2 BEAMS	4 BEAMS
2ANTENNAS	2A-2B	2A-4B	2A-2B	2A-4B
4ANTENNAS	4A-2B	4A-4B	4A-2B	4A-4B

In all simulations, $\frac{d}{\lambda} = \frac{1}{2}$, and the ML receiver resulted in the same SER performance as the maximum correlator receiver.

Based on (2.9), in BASK, the SER performance depends on the number of antennas and beams used in the system. Increasing the number of antennas (diversity order) and decreasing the number of beams (modulation level) reduces the SER for a given SNR in a manner comparable to the situation with conventional amplitude and phase modulations.

First, the BER results are presented for binary signaling with $M = 2$ in AWGN. In the BASK system, the AOA optimization to reduce the BER can be performed in

the transceiver training phase during the initial system startup, or when the system is re-initialized due to changes in channel conditions, e.g., reflector positions. To evaluate the BERs in different scenarios, both optimized and non-optimized AOAs were used.

For systems with two and four antennas, based on (2.11) and (2.12), the normalized distance was evaluated $\frac{d}{\sqrt{E_s}}$ and plotted in Figures 2.6 and 2.7, respectively, as a function of AOAs (φ_1 and φ_2). It can be seen that the inter-distances d_{ij} between spatial signatures increases when the number of antennas in the array increases. The peaks represent optimized angles resulting in lower SER.
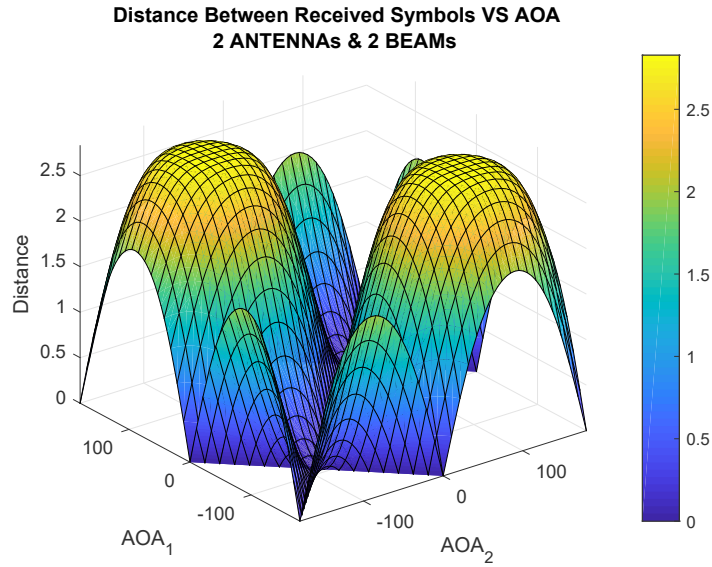
Figure 2.6: Distance in binary BASK as a function of AOAs, for $N_r = 2$.

From Figure 2.6, the maximum normalized distance is 2.83 (for $\varphi_1 = 90^o$ and $\varphi_2 = 271^o$), which implies a 3dB improvement in SNR when using BASK in an AWGN channel, as compared to BPSK with a single antenna receiver.

Based on the analytic expression in (2.9) and Figure 2.7 for the distance between two spatial signature vectors when $N_r = 4$, the normalized maximum distance $\frac{d_{min}}{\sqrt{E_s}} =$
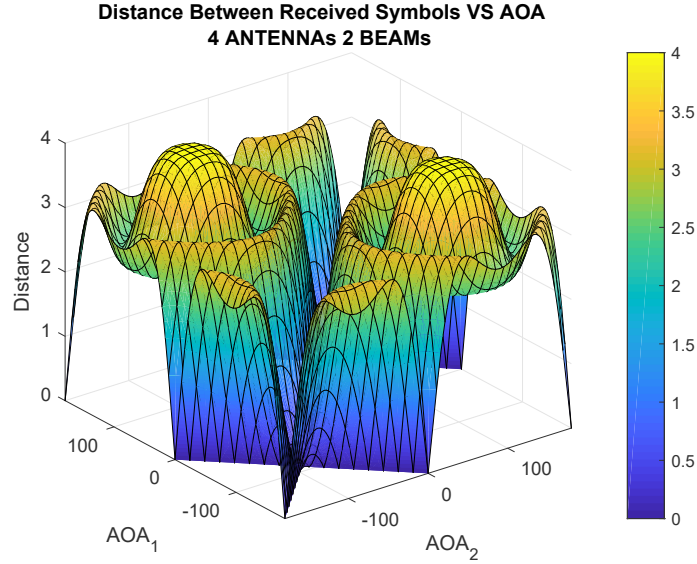
Figure 2.7: Distance in binary BASK as a function of AOAs, for $N_r = 4$.

4, with the same choice of $\varphi_1 = 90^o$ and $\varphi_2 = 271^o$ as when $N_r = 2$. When operating BASK in an AWGN environment with $N_r = 4$, this implies a 6dB SNR improvement over single antenna BPSK.

Figure 2.8 shows the BERs for a binary BASK system operating in an $AWGN$ channel with $N_r = 2$ and $N_r = 4$ antennas. The results are presented for optimized and non-optimized ($\varphi_1 = 35^o$ and $\varphi_2 = 60^o$) AOAs. In all cases, the simulations are in good agreement with the analytical results from the previous section, with distances evaluated according to the selected AOAs.

Secondly, the SER performance of a BASK system in an AWGN channel where $M = 4$ is considered. An exhaustive search optimization was performed to determine four AOAs (φ_1, φ_2, φ_3 and φ_4) that would maximize d_{min} as given in (2.13), based on inter-distances d_{ij} obtained from (2.9). In both cases, for $N_r = 2$ and $N_r = 4$, the optimum selection of AOAs is $\varphi_1 = 159^o$, $\varphi_2 = 89^o$, $\varphi_3 = 262^o$ and $\varphi_4 = 201^o$, resulting in maximized minimum distances of $1.34\sqrt{E_s}$ and $2.77\sqrt{E_s}$, respectively.
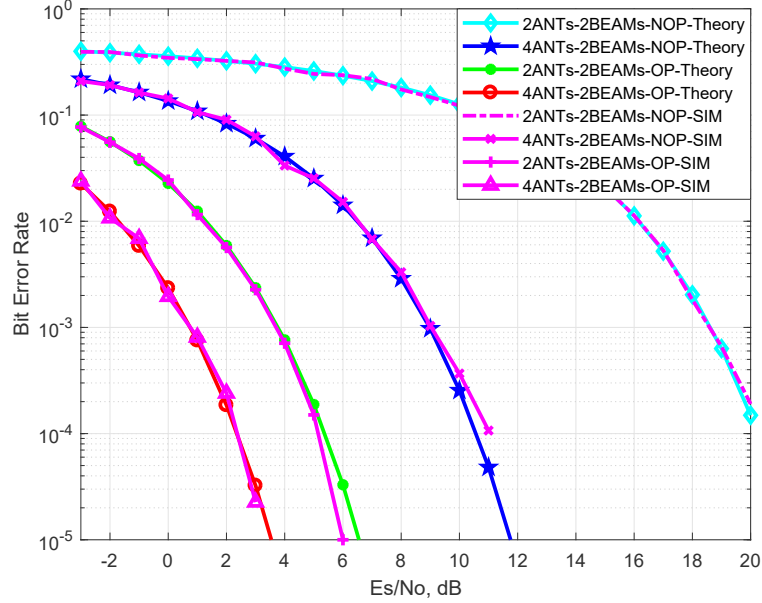
Figure 2.8: BER versus SNR in an AWGN channel, for binary BASK with $N_r = 2$ and $N_r = 4$, with optimized and non-optimized AOAs.

Figure 2.8 shows the SER for 4-ary BASK, which increases the bandwidth efficiency over that obtained for binary BASK. The results shown are for systems with optimized and non-optimized ($\varphi_1 = 20^o$, $\varphi_2 = 35^o$, $\varphi_3 = 60^o$ and $\varphi_4 = 85^o$) AOAs. Again, there is a good correlation between the simulated and analytical results. In the union upper bound in (2.9), it was necessary to consider $M_{min} = 2$ based on the number of signaling points at which the minimum distance was attained. Both Figures 2.8 and 2.9 indicate a significant performance gap between systems with optimized and non-optimized AOAs.

Thirdly, for an 8-ary BASK system in an AWGN channel, an exhaustive search optimization was also performed to determine eight AOAs that would maximize d_{min}. In both cases, where $N_r = 2$ and $N_r = 4$, the optimum AOAs were the same, resulting in maximized minimum distances of $0.72\sqrt{E_s}$ and $1.76\sqrt{E_s}$, respectively. To compare the SER performance of the proposed M-ary BASK with the performance of conventional
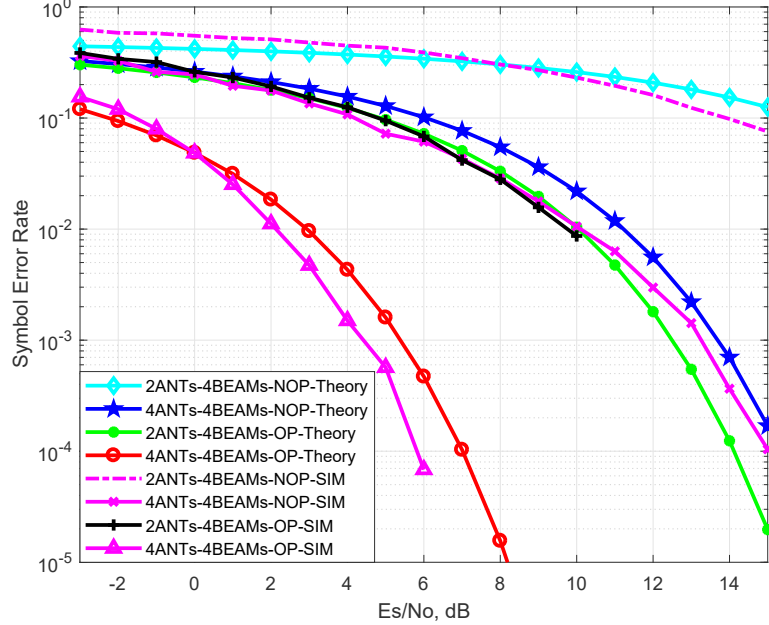
Figure 2.9: SER versus SNR in an AWGN channel, for 4-ary BASK with $N_r = 2$ and $N_r = 4$, with optimized and non-optimized AOAs.

M-ary pulse-amplitude modulation (PAM) in an AWGN channel, it should be recalled that in cases of M-ary PAM employed with a single-receiver antenna: (i) for $M = 4$, $SER_{4\text{-PAM}} \simeq \text{erfc}\left(\sqrt{\frac{E_s}{N_0} \cdot \frac{1}{5}}\right)$; and (ii) for $M = 8$, $SER_{8\text{-PAM}} \simeq \text{erfc}\left(\sqrt{\frac{E_s}{N_0} \cdot \frac{1}{21}}\right)$. The choice for comparison with PAM is both BASK and PAM as 1D modulations. For a fair comparison, it should be kept in mind that the discussions about BASK performance considered the SNR with a single-receiver antenna, whereas with M-ary PAM it is necessary to account for the fact that in a system with N_r receive antennas, the antenna diversity gain in AWGN (as compared to the single receive antenna case) is $10 \cdot \log_{10}(N_r)$. Based on these observations, M-ary BASK offers SNR gain improvements in different system configurations in comparison to M-ary PAM systems, as summarized in Table 2.5, where the second row of this table gives the normalized minimum distances for different configurations in a BASK system.

Table 2.5: SNR gain improvements in M-ary BASK as compared with M-ary PAM in an AWGN channel.

	$M = 2$		$M = 4$		$M = 8$	
	$N_r = 2$	$N_r = 4$	$N_r = 2$	$N_r = 4$	$N_r = 2$	$N_r = 4$
$\frac{d_{min}}{\sqrt{E_s}}$	2.83	4	1.34	2.77	0.72	1.76
SNR gain in dB	0	0	0.51	2.8	1.3	6.1

Finally, the SER performance for a BASK system in a Rayleigh fading channel is presented. Figure 2.10 shows the BER when $M = 2$ and Figure 2.11 shows the SER when $M = 4$.
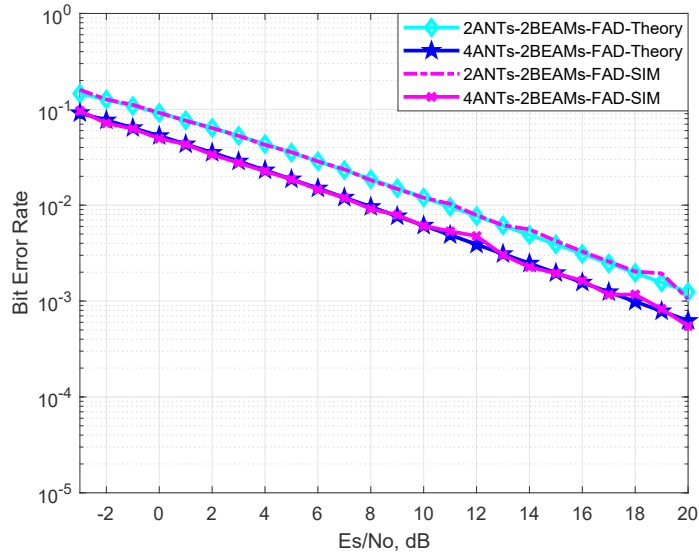
Figure 2.10: BER versus SNR in a Rayleigh fading channel for binary BASK, with $N_r = 2$ and $N_r = 4$ and optimized AOAs.
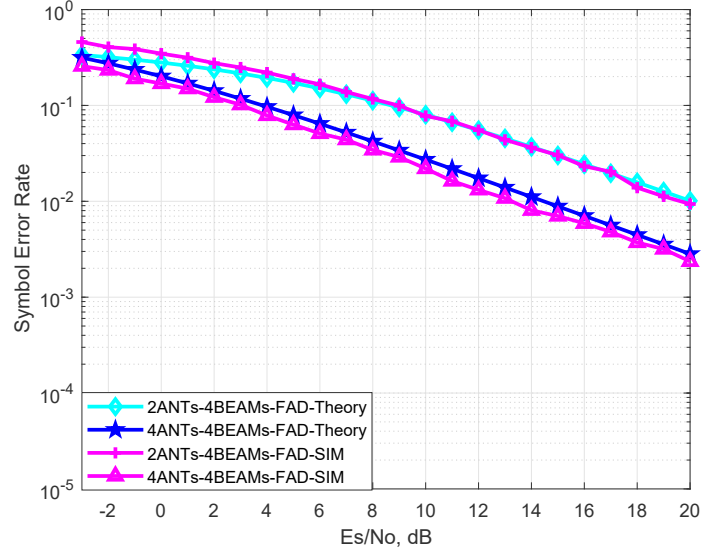
Figure 2.11: SER versus SNR in a Rayleigh fading channel for 4-ary BASK, with $N_r = 2$ and $N_r = 4$ and optimized AOAs.

Both figures illustrate the results only for optimized AOAs, and consider the two cases where $N_r = 2$ and $N_r = 4$. For binary signaling, there is excellent agreement between the simulated and analytical results for the BERs. When $M = 4$, the agreement is also good, although it should be understood that the analytical expressions in (2.8) and (2.14) represent only the union upper bound.

2.6   Summary

A multiple antenna transmission approach, referred to as beam angle shift keying (BASK), has been developed which employs smart antenna systems. The BASK system does not modulate the baseband signal. Rather, in a BASK system, spatial data directly modify the radiation patterns so that at the receiver, angular detection permits the recovery of the beamsteering index. The closed-form analytical performance of BASK in AWGN and Rayleigh fading channels has been derived. Moreover,

the simulation results have been shown to agree closely with analytical predictions. Methods of performance optimization have been suggested in terms of (i) AOA control during the training phase, and (ii) working with 3D channels including elevation angles. The proposed scheme works with a relatively small number of antennas for beamforming at the transmitter and the receiver and does not suffer from the limitations of similar schemes such as SSK, where the number of transmit antennas limits the modulation level.

3   Dual Layer Data Encoding Communication System

Chapter 2 presented principles of RF level modulation with an unmodulated carrier through indexing of transmitting/receiving beams. To further develop the proposed modulation scheme, this chapter introduces a transmission technique referred to as beam angle channel modulation (BACM) which uses a superposition of BASK and APM. In this scheme, rather than working with an unmodulated carrier signal as was the case with BASK, the scheme also encodes information into the amplitude and phase of the carrier signal. BACM utilizes the concept of a super symbol which is a combination of (i) an APM signal from the QAM or PSK constellation, and (ii) spatial symbol indexing of the transmitting/receiving beams.

In particular, at the encoder, the block of information bits from the super symbol is mapped into two symbols: (i) a spatial symbol selecting the direction of arrival of the amplitude- and phase-modulated carrier signal, and (ii) a temporal symbol chosen from the constellation diagram, such as QAM or PSK. The proposed scheme follows the model of concatenated modulation designs such as the recently introduced spatial modulation (SM), which is a generalization of SSK. The use of the transmitting RF carrier propagation angle through antenna array beamforming increases the spectral efficiency of single-input single-output (SISO) conventional (temporal) modulation by the base-two logarithm of the number of spatial beams that can be resolved (detected) at the receiver. The direction of arrival detection for spatial symbols is developed by

using a linear array of receive antennas. It is demonstrated that the reliability of detection of the spatial symbols in BACM is determined by the number of antennas used at the receiver and the actual angles of signal arrival.

The chapter is organized into six sections, to design data encoding and decoding for the BACM communication system, and to examine BACM performance through analytical derivations and simulations. Specifically, Section 3.1 discusses the proposed system model. Section 3.2 provides details about the dual layer modulation process. Section 3.3 presents the angle of arrival estimation method. Section 3.4 explains the detection process. Simulations and analytical results are demonstrated in Section 3.5. Finally, Section 3.6 summarizes the chapter.

3.1   Concatenated Modulation Technique

Concatenated modulation represents the concept of superposition of two different modulation schemes on one RF carrier to increase the spectral efficiency. This section presents the BACM concatenated modulation scheme and illustrates its operation with an example.

The BACM general system model is shown in Figure 3.1. Since BACM employs dual layer modulation, the encoder at the transmitter has two data paths: (i) the upper path represents the data encoded in QAM, or PSK modulation, and (ii) the lower path represents the data encoded into the transmitting beam pattern. In BACM, the transmitter uses one of M_s predetermined antenna array beams to send the complex QAM or PSK "temporal" symbol. The spatial symbols (S_k and $k \in \{1, 2 \cdots, M_s\}$, bearing information about $\log_2(M_s)$ data bits, index the beams following (if possible) conventional Gray mapping principles, i.e., the beams at the receiver that are most likely to be switched over (with the smallest Euclidean distance) differ by one spatial bit, as shown in Figure 3.2.
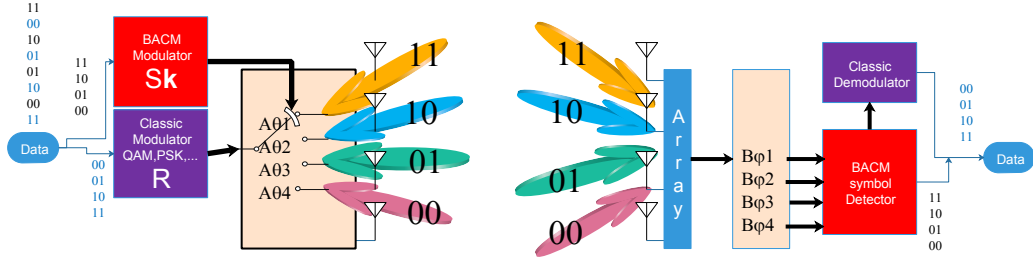
Figure 3.1: BACM concatenated modulation system.
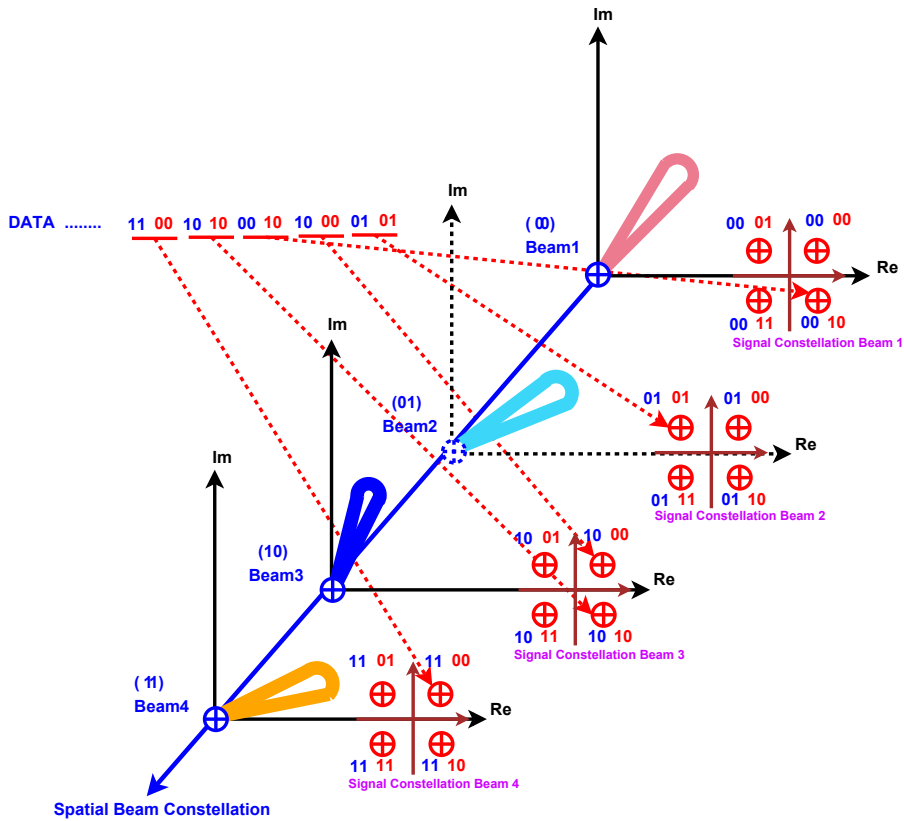
Figure 3.2: Illustration of BACM 3D encoding.

It is assumed that before the actual data transmission, there is a training phase involving the transmitter and the receiver. During the training phase, the receiver learns about (estimates) the M_s incoming signal directions φ_k, $(k = 1, ..., M_s)$, and it is assumed that these angles are known at the receiver during the detection phase.

The training phase could also be used to determine the selection of M_s transmitting beams from a larger set of radiation patterns so as to minimize the bit error rate (BER) for the spatial bits.

The BACM receiver uses an efficient direction-of-arrival (DOA) estimation algorithm to estimate and detect the incoming plane wave angle, φ_k, that represents the spatial symbol S_k in one-to-one mapping. The beams formed at the transmitter in the direction, θ_k, correspond to DOA φ_k. Without loss of generality, to simplify the description of the antenna models, it is assumed that linear and coplanar antenna arrays are used at both the transmitter and the receiver.

3.2 BACM Transmitter

In order to transmit a QAM or PSK signal $s(t)$ in a specific direction (θ_k, $\quad k = 1, \cdots, M_s$)) for the duration of one QAM/PSK symbol, the beamformer at the transmitter feeds the ith ($i = 1, \cdots, N_t$) antenna array element with $s(t)$ weighted by $A_{i\theta_k}$, to steer the beam in the direction θ_k, where N_t is the number of antennas at the transmitter. The beam steering vector mapper (BSVM) associated with each spatial symbol S_k yields a distinct direction-of-departure (DOD) beam angle θ_k. For an equally spaced linear array (with distance d between the antenna elements) as shown in Figure 3.3, when all the array elements are located on the x-axis and referenced to the array center point, the delay for the ith element is $\beta_i = -(N_t - 2 \cdot i + 1)\alpha\frac{d}{2}\sin(\theta)$, where α is the phase propagation factor given by $\frac{2\pi}{\lambda}$ and λ is the carrier wavelength. Hence, the steering vector defining the DOD angle θ_k (representing symbol S_k) can
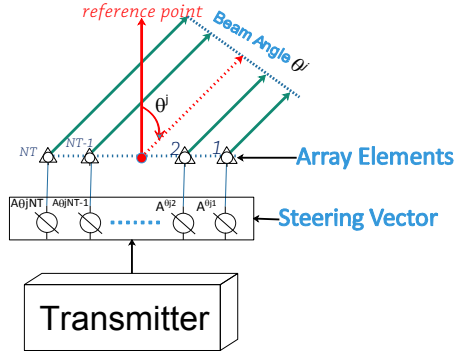
Figure 3.3: Transmitter antenna array.

be expressed as follows:

$$\mathbf{A}_{\theta_k} = \begin{bmatrix} e^{-j(N_t-1)\alpha\frac{d}{2}\sin\theta_k} \\[2ex] e^{-j(N_t-3)\alpha\frac{d}{2}\sin\theta_k} \\[2ex] \vdots \\[2ex] e^{j(N_t-3)\alpha\frac{d}{2}\sin\theta_k} \\[2ex] e^{j(N_t-1)\alpha\frac{d}{2}\sin\theta_k} \end{bmatrix} \tag{3.1}$$

After beamforming and phase shifting due to the delays β_i, in the direction θ_k, the signal radiated from the antenna array is a plane wave representing QAM or PSK symbols. While transmitting the QAM or PSK modulated signals, the beamformer selects the steering beam vector according to the spatial input symbol from the DOD/DOA mapper.

3.3 BACM Receiver

In the training phase, the BACM receiver determines the possible incoming signal angles φ_k and the one-to-one mapping between φ_k and S_k. This phase is followed by the data transmission phase, which first uses the DOA estimation/detection algorithm

to decide on the spatial symbols and then recovers the temporal symbols. To decide upon the DOA, i.e., one of the M_s known angles φ_k of the plane wave arriving at the receiver, a linear array with N_r elements is used, as shown in Figure 3.4, and a steering vector, $\mathbf{B}_{\varphi_k}$, is formed as follows:
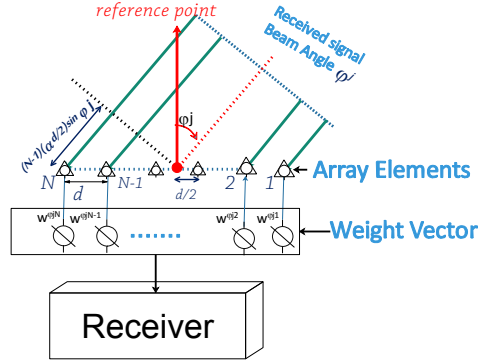
Figure 3.4: Receiver antenna array.

$$\mathbf{B}_{\varphi_k} = \begin{bmatrix} e^{-j(N_r-1)\alpha\frac{d}{2}\sin\varphi_k} \\[2ex] e^{-j(N_r-3)\alpha\frac{d}{2}\sin\varphi_k} \\[2ex] \vdots \\[2ex] e^{j(N_r-3)\alpha\frac{d}{2}\sin\varphi_k} \\[2ex] e^{j(N_r-1)\alpha\frac{d}{2}\sin\varphi_k} \end{bmatrix} \tag{3.2}$$

A steering vector serves as a form of MRC receiver for received signals at the ith $(i = 1, \cdots, N_r)$ element scaled by

$$e^{j2\pi \cdot f_c \cdot \beta_i}$$

with

$$\beta_{\pm i} = \pm i \times \frac{d}{2} \cdot \sin(\varphi_k) \qquad i = \begin{cases} \{1, 3, 5, \cdots, \frac{N_r}{2} + 1\} & N_r \ even \\[2ex] \{0, 2, 4, \cdots, \frac{N_r+1}{2}\} & N_r \ odd \end{cases}$$

representing the delay for the kth transmitting beam. Based on all M_s possible beam angles, the receiver forms a set of steering vectors matched to the M_s possible received vector signals impinging on the receive antenna array and arranges them in a matrix hereafter referred to as the detection matrix (DM):

$$\mathbf{D} = \begin{bmatrix} e^{-j(N_r-1)\alpha\frac{d}{2}\sin\varphi_1} & \cdots & e^{-j(N_r-1)\alpha\frac{d}{2}\sin\varphi_{M_s}} \\ e^{-j(N_r-3)\alpha\frac{d}{2}\sin\varphi_1} & \cdots & e^{-j(N_r-3)\alpha\frac{d}{2}\sin\varphi_{M_s}} \\ \vdots & & \vdots \\ e^{-j\alpha\frac{d}{2}\sin\varphi_1} & \cdots & e^{-j\alpha\frac{d}{2}\sin\varphi_{M_s}} \\ e^{j\alpha\frac{d}{2}\sin\varphi_1} & \cdots & e^{j\alpha\frac{d}{2}\sin\varphi_{M_s}} \\ \vdots & & \vdots \\ e^{j(N_r-1)\alpha\frac{d}{2}\sin(\varphi_1} & \cdots & e^{j(N_r-1)\alpha\frac{d}{2}\sin\varphi_{M_s}} \end{bmatrix} \tag{3.3}$$

which, in a column representation, appears as:

$$\mathbf{D} = \begin{bmatrix} \mathbf{B}_{\varphi_1} & \mathbf{B}_{\varphi_2} & \cdots & \mathbf{B}_{\varphi_{M_s}} \end{bmatrix} \tag{3.4}$$

As the name implies, the detection matrix is used in various detection algorithms to detect the angle of arrival representing the spatial symbols. After the training phase, $\mathbf{B}_{\varphi_k}$ are known via estimation of all the angles of arrival (AOA) during the training phase, by using methods such as multiple signal classification (MUSIC). The steering vectors $\mathbf{B}_{\varphi_k}$ can also be calculated by observing the phase shifts of the known transmitted symbols (assuming that the difference between the delays along different paths does not span more than a fraction of the duration of the temporal symbol).

3.4 Detection Process

There are several methods for detecting the DOAs when the possible AOAs are known, e.g., maximum likelihood, or classifiers based on parametric models such as MUSIC, with the latter requiring multiple snapshots of the received signal vector [54]. These methods differ in performance, which may result from different levels of computational complexity. Here, only one method is examined, that depends on taking a single snapshot (in the spatial domain) of the vector signal at the receiving array after downconversion and matched filtering of signals from all antenna elements. For clarity of presentation, the initial consideration will involve (i) only two AOAs, φ_1 and φ_2 (corresponding to two spatial symbols S_1, S_2 with $M_s = 2$), and (ii) a detection process with the BACM receiver using $N_r = 4$ antenna elements, as shown in Figure 3.5.
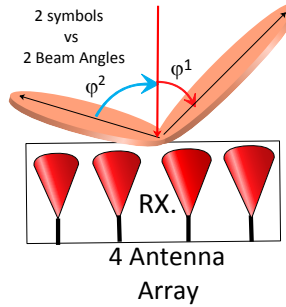
Figure 3.5: Signals impinging on the receive antenna array.

At the transmitter, the two steering beams $\mathbf{A}_{\theta_1}$ and $\mathbf{A}_{\theta_2}$, according to (3.1), are employed. However, these vectors and their size do not influence the detection process if the arriving signal is a plane wave. Based on the arrival angles estimated during

the receiver training session, the receiver forms the following steering vectors:

$$
\mathbf{B}_{\varphi_1} =
\begin{bmatrix}
e^{-j3\alpha\frac{d}{2}\sin\varphi_1} \\
\\
e^{-j\alpha\frac{d}{2}\sin\varphi_1} \\
\\
e^{j\alpha\frac{d}{2}\sin\varphi_1} \\
\\
e^{j3\alpha\frac{d}{2}\sin\varphi_1}
\end{bmatrix}
\quad
\mathbf{B}_{\varphi_2} =
\begin{bmatrix}
e^{-j3\alpha\frac{d}{2}\sin\varphi_2} \\
\\
e^{-j\alpha\frac{d}{2}\sin\varphi_2} \\
\\
e^{j\alpha\frac{d}{2}\sin\varphi_2} \\
\\
e^{j3\alpha\frac{d}{2}\sin\varphi_2}
\end{bmatrix}
\tag{3.5}
$$

These are matched to two possible discrete vector (information bearing) signals arriving from two possible directions:

$$
\mathbf{R}_x = R \cdot
\begin{bmatrix}
e^{-j3\cdot2\pi\cdot f_c\cdot\alpha\frac{d}{2}\sin\varphi_x} \\
\\
e^{-j\cdot2\pi\cdot f_c\cdot\alpha\frac{d}{2}\sin\varphi_x} \\
\\
e^{j\cdot2\pi\cdot f_c\cdot\alpha\frac{d}{2}\sin\varphi_x} \\
\\
e^{j3\cdot2\pi\cdot f_c\cdot\alpha\frac{d}{2}\sin\varphi_x}
\end{bmatrix}
+ \mathbf{N}
\tag{3.6}
$$

where $x = 1$ or $x = 2$ for $M_s = 2$; $(\cdot)^T$ stands for the matrix transpose; and $\mathbf{N} = [n_1, \cdots, n_{N_r}]^T$, with n_i representing independent and identically distributed (i.i.d.) AWGN at the ith antenna. The transmitted QAM/PSK scalar symbol R is fixed for the symbol duration, which permits detection to be decoupled for the spatial and temporal symbols.

Maximum Ratio Combining

This method uses linear (weighted) combining of signals from different antenna elements. The weighting vectors $\mathbf{w}_{\varphi_k}$, multiplying the received vector $\mathbf{R}_x$, are chosen to maximize the SNR of the combined signal output. This SNR is maximized when:

$$
\mathbf{w}_{\varphi_k} = \mathbf{B}_{\varphi_k}^{H}
\tag{3.7}
$$

where $(\cdot)^H$ represents the Hermitian transpose [15].

To obtain the decision variables to discriminate between φ_1 and φ_2, the detection matrix (DM) is formed: $\mathbf{D} = \begin{bmatrix} \mathbf{B}_{\varphi_1} & \mathbf{B}_{\varphi_2} \end{bmatrix}$. The receiver uses the DM to detect the angle of arrival of the received signal in an unknown direction φ_x ($x = 1$ or $x = 2$), which is one of the M_s possible steering angles. The DM thus also detects the "spatial" symbol. Without accounting for AWGN effects and fading, the decision variable $\mathbf{X}$ is formed by applying the DM to the received vector signal $\mathbf{R}_x$ as follows:

$$\mathbf{X} = \boldsymbol{D}^H \cdot \mathbf{R}_x = R \cdot \boldsymbol{D}^H \cdot \mathbf{B}_{\varphi_x} = R \cdot \begin{bmatrix} \mathbf{B}_{\varphi_1} & \mathbf{B}_{\varphi_2} \end{bmatrix}^H \begin{bmatrix} \mathbf{B}_{\varphi_x} \end{bmatrix} \tag{3.8}$$

where $\varphi_x \in \{\varphi_1, \varphi_2\}$. Based on (3.2),

$$\mathbf{X} = R \cdot \begin{bmatrix} \mathbf{B}_{\varphi_1}^H \\ \\ \mathbf{B}_{\varphi_2}^H \end{bmatrix} \begin{bmatrix} \mathbf{B}_{\varphi_x} \end{bmatrix} = R \cdot \begin{bmatrix} \mathbf{B}_{\varphi_1}^H \, \mathbf{B}_{\varphi_x} \\ \\ \mathbf{B}_{\varphi_2}^H \, \mathbf{B}_{\varphi_x} \end{bmatrix} \tag{3.9}$$

and the coordinate with the largest real part decides upon the transmitted spatial symbol. It has been tacitly assumed so far that the signals arriving from different directions have the same energy $E_s = 1$ at every receive antenna element. If this is not the case, as determined during the training phase, the weight vectors $\mathbf{A}_{\theta_k}$ at the transmitter can be adjusted to satisfy this condition.

In the AWGN channel, the maximum correlator receiver developed is the ML receiver for spatial symbols. It projects the received signal $\mathbf{R}_x$ onto all possible spatial signature vectors $\mathbf{B}_{\beta_k}$ ($k \in \{1, \cdots, N_r\}$) and decides on the index resulting in the maximum correlation. In the absence of noise, the maximum absolute value in (3.9) is equal to $N_r \cdot |R|$. This is when $\varphi_x = \varphi_k$, with φ_k representing the actual AOA. The other element in $\mathbf{X}$ is $R \cdot \mathbf{B}_{\varphi_2}^H \cdot \mathbf{B}_{\varphi_1}$. From the Schwartz inequality, $|\mathbf{B}_{\varphi_2}^H \cdot \mathbf{B}_{\varphi_1}| \leq N_r$. Eventually, it is the Euclidean distance between the complex vectors $\mathbf{B}_{\varphi_2}$ and $\mathbf{B}_{\varphi_1}$ (for

$M_s = 2$) that determines the symbol error rate (SER) and the BER for the spatial symbols/bits. This is presented in the next section.

3.5 Performance Analysis and Simulation Results

This section provides analytical and simulation results for evaluating the performance of the proposed BACM system in an AWGN channel.

In order to optimize the BER for spatial symbols, the behavior of the decision variables in $\mathbf{X}$, as given in (3.9), could be analyzed. However, in the absence of AWGN, the SER for the spatial symbols (SER_{spatial}) depends upon the minimum Euclidean distance $d_{min,spatial}$ between the received vector signal representations, as in (3.4), i.e.,

$$d_{min,spatial} = \min\left(\sqrt{E_s} \cdot \left\|\vec{\mathbf{B}}_{\varphi_i} - \vec{\mathbf{B}}_{\varphi_j}\right\|\right)$$

over all $i \neq j$, where $\|\cdot\|$ is the L_2 norm of a vector.

Specifically, SER_{spatial} could be upper bounded in the AWGN channel as [15]:

$$SER_{\text{spatial}} \simeq \frac{M_{min}}{2}\text{erfc}\left(\sqrt{\frac{d^2_{min,spatial}}{4 \cdot N_0}}\right) \tag{3.10}$$

where erfc($\cdot$) is the complementary error function, N_0 is the noise power spectral density (PSD), and M_{min} is the number of points in the constellation reached with the minimum distance from the perspective of any point that results in a maximum of these numbers. In determining $d_{min,spatial}$ for $N_r = 4$, the normalized inter-distances

$\frac{d_{ij}}{\sqrt{E_s}}$ between spatial signature vectors $\mathbf{B}_{\varphi_i}$ and $\mathbf{B}_{\varphi_j}$ are calculated as:

$$\frac{d_{ij}}{\sqrt{E_s}} = \left\| \vec{\mathbf{B}}_{\varphi_i} - \vec{\mathbf{B}}_{\varphi_j} \right\| = \left\| \begin{array}{c} e^{-j3\beta_i} - e^{-j3\beta_j} \\\\ e^{-j\beta_i} - e^{-j\beta_j} \\\\ e^{j\beta_i} - e^{j\beta_j} \\\\ e^{j3\beta_i} - e^{j3\beta_j} \end{array} \right\| \tag{3.11}$$

where

$$\beta_i = \frac{2\pi}{\lambda} \cdot \frac{d}{2} \cdot \sin(\varphi_i) \tag{3.12}$$

When only two beams are used (determined by DOA φ_1 and φ_2 for $M_s = 2$), and when $N_r = 4$, the distance $d_{min,spatial} = d(\varphi_1, \varphi_2)$ is a function of two variables:

$$d = \sqrt{E_s} \sqrt{2 \left((\cos \beta_1 - \cos \beta_2)^2 + ... + (\sin 3\beta_1 - \sin 3\beta_2)^2 \right)} \tag{3.13}$$

Assuming that $E_s = 1$, this distance is plotted (for $d = \frac{\lambda}{2}$) in Figure 3.6 as a function of φ_1 and φ_2, in the range $[-180°, 180°]$ for both of them. In consideration of the symmetry of the problem, clearly $\varphi_1 = \varphi_2$ and $\varphi_1 + \varphi_2 = -180°$ should be avoided, since these are not distinguishable DOAs. In addition, there are some pairs of (φ_1, φ_2) that maximize the distance, resulting in lower SER_{spatial} (for $M_s = 2$ $SER_{\text{spatial}} = BER_{\text{spatial}}$ and $M_{min} = 1$).

This issue can be examined further by fixing φ_1 and plotting slices $d'(\varphi_2) = d(\varphi_1, \varphi_2)$ by using (3.13), as shown in Figures 3.7 and 3.8 for $\varphi_1 = 95°$ and $\varphi_1 = 20°$, respectively. To maximize the separation between spatial signature vectors, when $\varphi_1 = 95°$, φ_2 should be adjusted to $-90°$, and when $\varphi_1 = 20°$, φ_2 should be $-23°$. In the first case, for $E_s = 1$, the maximum separation between spatial signature vectors that minimizes BER_{spatial} is 4, and in the second case it is 3.19. By analyzing equivalents of (3.13), it was determined that the higher the number of antennas at
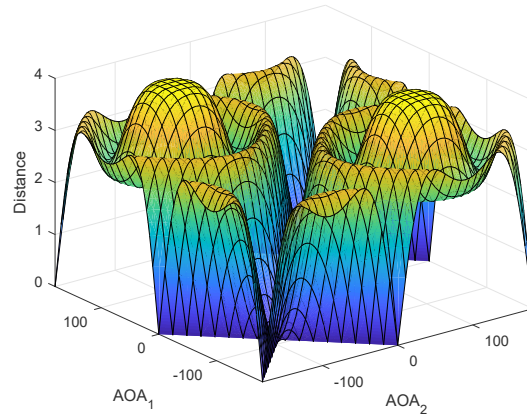
Figure 3.6: Distances between spatial signature vectors versus possible AOAs.

the receiver, the greater the separation between spatial signature vectors, resulting in lower SER_{spatial}.
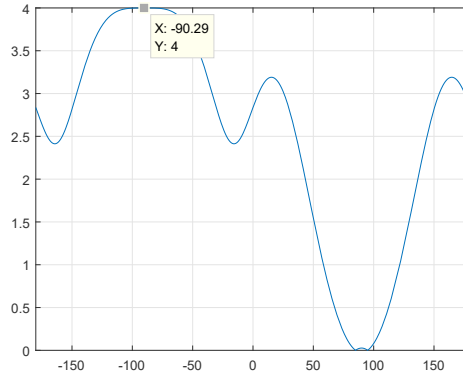
Figure 3.7: Slice of distances between spatial signature vectors versus possible AOAs, for φ_2 when $\varphi_1 = 95°$.

Based on the number of antennas at the receiver and the spatial modulation level M_s, which determines the number of required beam angles, an optimization procedure could be developed following the above approach. This would have the purpose of fine-tuning the choice of $\varphi_1, \cdots \varphi_{M_s}$ so as to maximize $d_{min,spatial}$, to reduce SER_{spatial}. This could be exploited in the training phase, when the transmitter and receiver decide
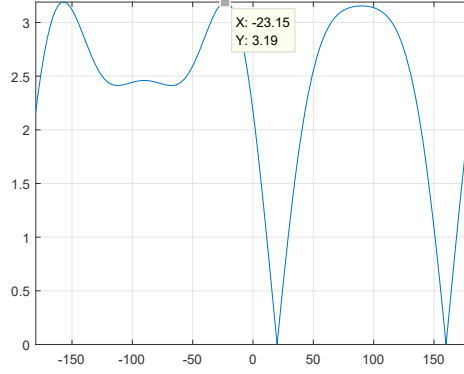
Figure 3.8: Slice of distances between spatial signature vectors vs possible AOAs for φ_2 when $\varphi_1 = 20°$.

which AOAs are to be utilized.

To examine the performance of BACM, Matlab® was used to simulate the BERs in the proposed system for an AWGN channel. For the spatial data path, binary signalling was used, while for the temporal data path, QPSK was used. In the simulation, the receiver includes a uniform linear array (ULA) with $N_r = 4$ antennas spaced at $d = \frac{\lambda}{2}$. The AOAs are adjusted to $\varphi_1 = 95°$ and $\varphi_2 = -90°$ to achieve the maximum separation in the spatial dimension. Figure 3.9 shows the BER of the underlying system for temporal (QPSK) and spatial bits as a function of SNR (per antenna). For comparison purposes, the BER is also shown as a function of SNR for a conventional SISO system in an AWGN channel. (Here, when $M_s = 2$, for the spatial bits $E_b = E_s$.) Good agreement was observed between the BER simulated for the spatial bits (represented by the black curve with triangles) and the theoretical BER_{spatial} (represented by the red curve with circles), as given in (3.10) (with $M_{min} = 1$) and based on (3.13) and (3.12). Furthermore, with the receiver beamforming weights chosen and the optimized AOAs, the BERs for the spatial and temporal bits (the dashed blue curve) are comparable, which may not always be the case, especially if the AOAs are not optimized.
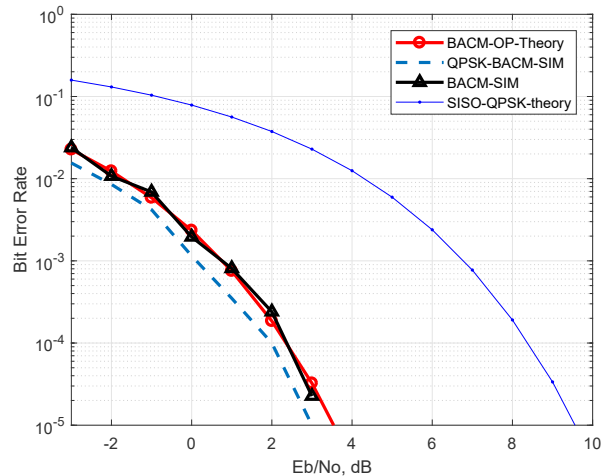
Figure 3.9: BER versus Eb/No in AWGN for spatial (BACM) and temporal (BACM QPSK) bits, when $N_r = 4$.

Finally, for a fair comparison, it must be kept in mind that the SNR was considered for a single-receiver antenna, while for the QPSK used to represent the temporal bits it should be taken into account that in a system with N_r receive antennas, the antenna diversity gain in AWGN (as compared to the single receive antenna case) is $10 \log_{10}(N_r)$. This is the reason why there is a 6dB gain for temporal bits in comparison to the SISO QPSK modulation, which means that this cannot be claimed as a diversity gain. However, SISO QPSK has a 2 bps/Hz bandwidth efficiency, while the BACM system in the configuration analyzed in this section has a bandwidth efficiency of 3 bps/Hz. In general, in the proposed system with M-ary PSK or M-ary QAM in the temporal data path and M_s AOAs in the spatial data path, the bandwidth efficiency is $\log_2(M) + \log_2(M_s)$ bps/Hz. The power efficiency is determined by the AOAs and the number of receive antennas.

3.6   Summary

A novel transmission technique referred to as beam angle channel modulation (BACM) has been presented in this chapter. BACM uses an antenna array to encode spatial symbols into the angle of propagation (and arrival) of an amplitude- and phase-modulated carrier. This 3D modulation scheme is a concatenation of two modulations. First, at the baseband, a "temporal" symbol modulates the phase and amplitude of the carrier. Then a spatial symbol indexes the DOD of the transmitter radiation pattern, as in BASK. The concatenation of 'temporal"/APM and spatial symbols results in the transmission of a super symbol, which in turn increases the spectral efficiency of single-input single-output (SISO) conventional (temporal) modulation by the base-two logarithm of the number of spatial beams that can be resolved (detected) at the receiver. The closed-form analytical performance of BACM in AWGN channels has been derived and simulation results have been shown to agree closely with the analytical predictions. Research directions for performance optimization have been suggested.

To compensate for BER performance losses, BACM can employ more advanced array signal processing strategies such as multiple snapshots for DOA detection. BACM thus has the potential to satisfy a diverse range of practical requirements, which will necessitate further investigation.

4   Multiple Access Based on Beam Angle Shift Keying

This chapter extends the beam angle shift keying (BASK) transmission technique into a multiuser version referred to as beam angle multiple access (BAMA). Multiple access on the uplink is achieved by assigning subsets of beams to individual users signaling with BASK. At the base station, for the duration of the spatial symbol, the receiver decides on a subset of possible multiple AOAs corresponding to synchronized spatial symbols from different users. Specifically, a maximum likelihood (ML) detector is proposed that can successfully decode incoming data from multiple simultaneous BASK transmissions by employing a linear array of receiving antennas. Unlike the situation in spatial division multiple access, where a fixed beam arrangement is used, BAMA detects the beams utilized by multiple users on a symbol-by-symbol basis. In the proposed scheme, beam management and selection are crucial with respect to the capacity of the system. It is demonstrated that the reliability of detection of the spatial symbols in BAMA is determined by the number of antennas used at the receiver and the actual angles of signal arrival.

This chapter is organized as follows: The system model for the proposed multiple access system is described in Section 4.1. The design of the suggested receiver is presented in Section 4.2. In Section 4.3, the simulation results are illustrated for both optimized and non-optimized beam angles. Finally, Section 4.4 summarizes the chapter.

4.1   System Model

To accomplish multiple access communication on the uplink based on BASK, the receiver uses a multi-beam smart antenna array which detects N directional beams concurrently at the base station (BS), where N is the number of users. For every symbol duration, each user utilizes one radiation beam to encode data. It is assumed that users are synchronized when their symbols, represented by the beams, arrive at the BS. The total number of beams M is:

$$M = \sum_{i=1}^{N} M_i \qquad (4.1)$$

where M_i is the number of symbols/beams for user i, although, when detection is performed, only N of these beams are active. By detecting groups of N beams, the BAMA system decodes data of N users. Figure 4.2 illustrates the system for two users, with two beams per user, so that $N = M_1 = M_2$ and $M = 4$. The proposed concept generalizes beam angle shift keying (BASK) modulation to the multiuser case. In BASK modulation, the transmitted data is encoded in the RF wave propagation direction for the channel. By detecting the direction of arrival, the receiver can decode the data. In BASK, temporal modulation can be used to add another layer of data to the transmitted signal in order to construct a concatenated modulation (multilayer) system to increase bandwidth efficiency, as described in Chapter 2 [18]. Here, only the unmodulated carrier is used, as explained in Chapter 1 [17].

As shown in Figure 4.1, the signal R_i received from each user in direction φ_i for each antenna element passes through a weighting process to compensate for the delay θ_i that is associated with the angle of arrival φ_i. This determines the angle of arrival φ_{x1} and φ_{x2}, and could follow a process similar to that presented in Sections 1.3.2 and 1.3.4. The following section describes the multiuser version of the BASK receiver in more detail.
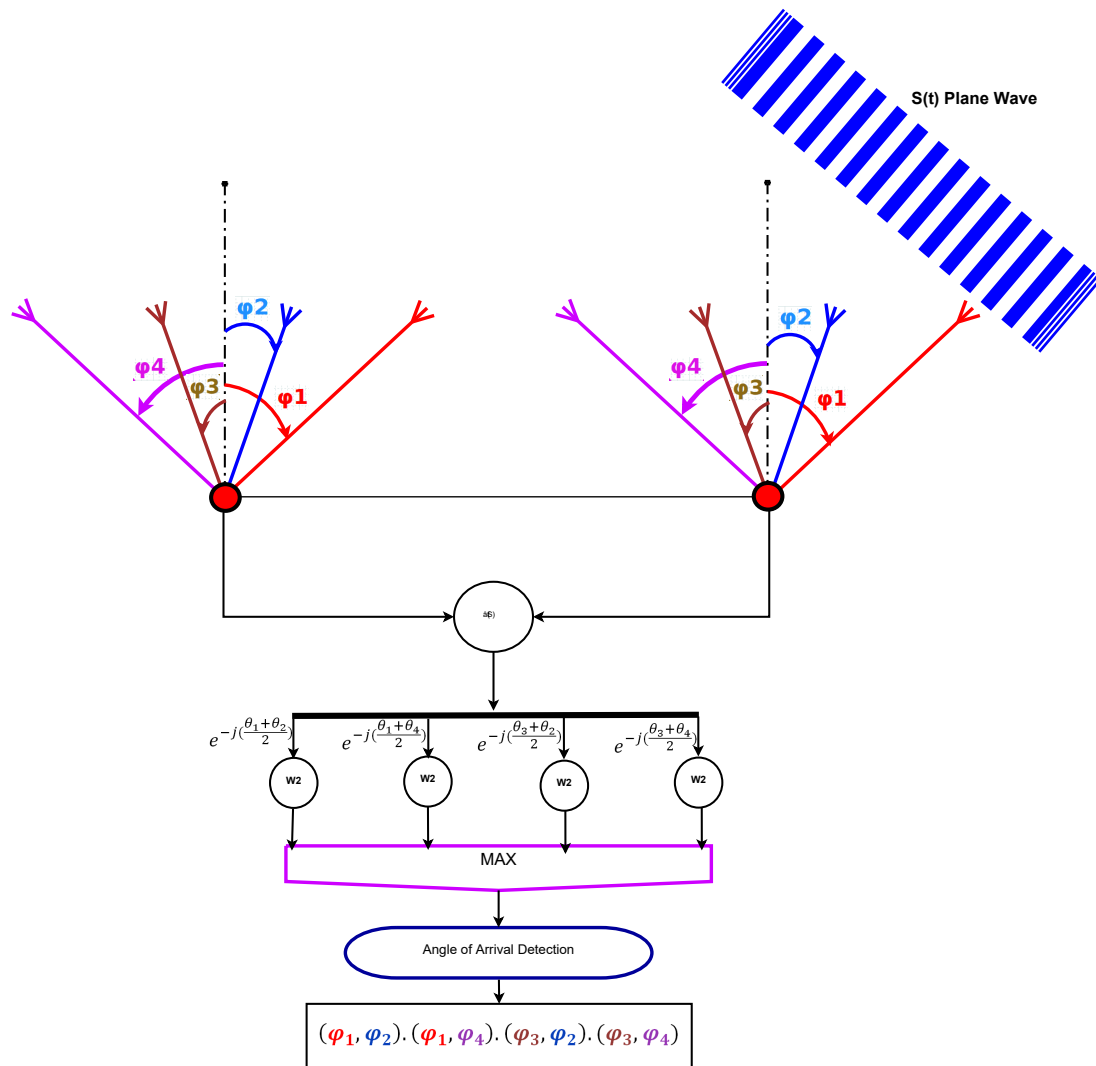
Figure 4.1: BAMA in a MIMO channel environment.

4.2 Multi-Beam Multiuser Receiver

4.2.1 Description

A proper phase compensation to ensure in-phase combining of the received signals in direction φ_k, results in higher signal strength at the receiver output. Therefore, to detect the relevant AOA among possible AOAs, as per Table 4.1, the receiver

Table 4.1: Possible AOA combinations for two users signaling with BASK.

	USER 2 (AOA)	
	ϕ_2	ϕ_4
USER 1 ϕ_1	$\phi_1\phi_2$	$\phi_1\phi_4$
(AOA) ϕ_3	$\phi_3\phi_2$	$\phi_3\phi_4$

applies all possible compensation weightings and selects the corresponding AODs that generate the maximum signal strength at the output.

4.2.2 Downlink

The base station exploits adaptive antennas to transmit in M directions, where M is the aggregation of the number of symbols or required beam angles (BA) for users 1 to N. Assuming that the BS in Figure 4.2 transmits one bit per symbol (similar to BPSK) to two separate users (user 1 and user 2), then $M = 4$, i.e., there are four transmission directions at the base station (BS) on a downlink. In each time slot, the base station chooses two of four beams, based on the symbols transmitted for the two users. Thus, in general, the transmitter chooses N beams from M available beams to communicate simultaneously with N users. When receiving on the downlink, user i decides on one beam from the M_i angles designated for this user.

4.2.3 Uplink

The main focus of this research is on the uplink part of the proposed system. Let us consider a wireless communication system with a base station and N users. For simplicity, assume that $N = 2$, i.e., there are two users, as shown in Figure 4.2. The proposed system has three main features:

1. The base station and all users utilize adaptive antennas, to be able to have

multiple beam angles in the propagation pattern, i.e., transmitting and receiving in multiple directions.

2. For communication, the base station and users employ a single frequency carrier signal with no modulation. This is one of the advantages of this system that makes it unique in terms of bandwidth efficiency improvement in comparison to other multiple access systems.

3. The system has the advantage of a higher signal-to-noise ratio as a result of using antenna array producing RF directional gain.
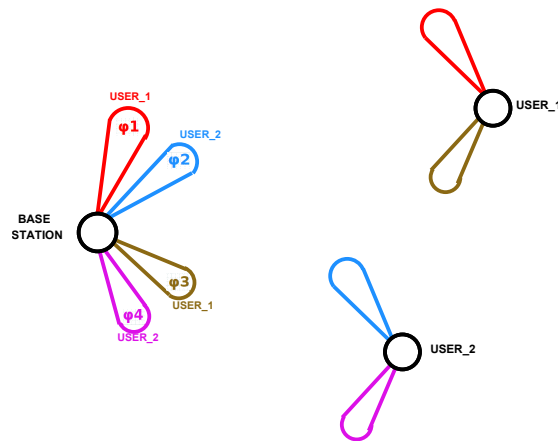
Figure 4.2: Multiple access with multiple beams.

In this multiple access system, for the uplink, all users transmit data that is encoded into the beam angle of the transmitted signal or direction of departure. For the system illustrated in Figure 4.2 that consists of two users, at each time slot, simultaneously, user 1 transmits a single frequency signal in one of the two predetermined directions φ_1 or φ_3, and user 2 transmits a single frequency signal in one of the two predetermined directions φ_2 or φ_4. Table 4.1 shows the possible signal direction combinations at different data time slots. Specifically, in this setup for two

users, the base station (uplink) receives two signals in two different directions on the same frequency, in four possible combinations of beams.

4.2.4 Detection

This section focuses on the detection process for the received signal in the BS. Without loss of generality, the beam angle multiple access system illustrated in Figure 4.2 is considered. This system consists of two users, and the BS utilizes a uniform linear array (ULA) antenna with two elements, as shown in Figure. 4.3:

$$User\,1 \begin{cases} \varphi_1 \\ \\ \varphi_3 \end{cases} \qquad User\,2 \begin{cases} \varphi_2 \\ \\ \varphi_4 \end{cases}$$

In order to detect the data in the uplink, the base station should detect the beam arrival angle for each user, among the predetermined directions that are designated for each symbol in the training phase of the initial link setup.
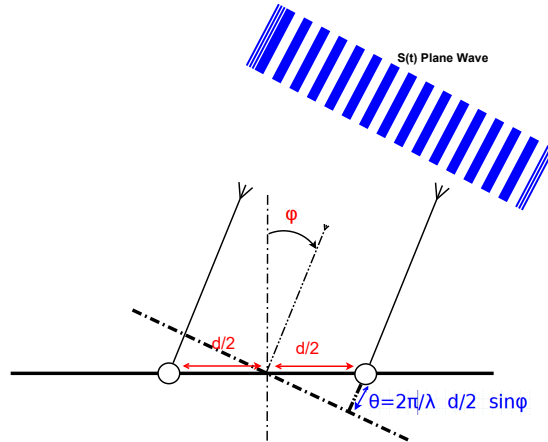
Figure 4.3: Uniform linear antenna array.

For a single plane wave $S(t)$ arriving from direction φ, the signal delay θ, referenced

to the array center point at the input of the array combiner, can be obtained as follows:

$$\theta = \frac{2\pi}{\lambda} \frac{d}{2} \sin \varphi \tag{4.2}$$

Without loss of generality, assume $d = \lambda$. Therefore, in general, the delay related to the angle of arrival φ for any user is:

$$\theta = \pi \sin \varphi \tag{4.3}$$

For the detection in the presence of AWGN, we could use ML detectors, matching the received signals vector to all possible valid codewords and find the received spatial symbol in each direction separately. However, here to obtain higher resolution when the difference between the angle of arrivals is small, which result in performance degradation, we work with the combined signals from both antenna elements. Initially, noise effects are disregarded and a high signal-to-noise ratio (SNR) environment is assumed; the analysis is later extended to a noisy channel. The output of the antenna array when two signals from two users arrive in unknown directions φ_{x1} for user 1 and φ_{x2} for user 2 is as follows:

$$\mathbf{R} = \begin{bmatrix} R_1(t) \\ R_2(t) \end{bmatrix} = \begin{bmatrix} e^{j\theta_{x1}} & e^{j\theta_{x2}} \\ e^{-j\theta_{x1}} & e^{-j\theta_{x2}} \end{bmatrix} \begin{bmatrix} S_1(t) \\ S_2(t) \end{bmatrix} \tag{4.4}$$

where $S_1(t)$ and $S_1(t)$ are the plane waves arrived at the receiver from two directions determined by θ_1 and θ_2; also $R_1(t)$ and $R_2(t)$ are the received signals at antenna one and antenna two respectively. To simplify the operation of the receiver and to use generic ML detector, we are going to deploy the combined signals from individual antennas. At the output of the receiving antenna array combiner, the combined signals from individual elements can be expressed as:

$$R(t) = S_1(t)\left(e^{j\theta_{x1}} + e^{-j\theta_{x1}}\right) + S_2(t)\left(e^{j\theta_{x2}} + e^{-j\theta_{x2}}\right) \tag{4.5}$$

Assuming that we have a power control algorithm, so both received signals have the same power level, and $S_1(t) = S_2(t) = \sqrt{E_s}e^{j2\pi f_c t}$.

In a general form for an N_r element antenna array and two users, assuming $\sqrt{E_s} = 1$ the output of the antenna array combiner (4.5) can be expanded as:

$$R(t) = \sum_{k=2,4,\ldots}^{N_r} \left[e^{j(2\pi f_c t + (k-1)\theta_{x1})} + e^{j(2\pi f_c t - (k-1)\theta_{x1})} \right. \tag{4.6}$$

$$\left. + e^{j(2\pi f_c t + (k-1)\theta_{x2})} + e^{j(2\pi f_c t - (k-1)\theta_{x2})} \right]$$

$$R(t) = k \sum_{k=2,4,\ldots}^{N_r} \left[\cos(2\pi f_c t + (k-1)\theta_{x1}) + \cos(2\pi f_c t + (k-1)\theta_{x2}) \right] \tag{4.7}$$

In a special case for two users, the signal at the nth antenna element to the left and right of the reference point can be represented as:

$$\begin{aligned} R_{n1}(t) + R_{n2}(t) &= 2\left[\cos(2\pi f_c t + (n-1)\theta_{x1}) + \cos(2\pi f_c t + (n-1)\theta_{x2}) \right] \\ &= 4\cos\left(\frac{(n-1)(\theta_{x1} - \theta_{x2})}{2} \right) \cos\left(2\pi f_c t + \frac{(\theta_{x1} + \theta_{x2})}{2} \right) \quad (4.8) \\ &= K\cos\left(2\pi f_c t + \frac{(\theta_{x1} + \theta_{x2})}{2} \right) \end{aligned}$$

The above equation implies that when two signals arrive at the antenna array from two different angles φ_{x1} and φ_{x2}, with the corresponding delays θ_{x1} and θ_{x2} (at the same time and same frequency), this is equivalent to a signal arriving at a virtual angle of arrival (VAOA) φ_v associated with a virtual delay θ_v:

$$\theta_v = \frac{(\theta_{x1} + \theta_{x2})}{2} \tag{4.9}$$

Substituting (4.3) in (4.9) results in:

$$\theta_v = \frac{\pi(\sin\varphi_{x1} + \sin\varphi_{x2})}{2} \tag{4.10}$$

and finally:

$$\varphi_v = \arcsin\left(\frac{\sin\varphi_{x1} + \sin\varphi_{x2}}{2}\right) \tag{4.11}$$

This result is used to design a receiver to distinguish between multiuser signals on the uplink, as shown in Figure 4.1. The maximum correlation receiver (MCR) projects the combined received signals, $R_1(t) + R_2(t)$, into all possible spatial signature vectors, and decides upon the combination that results in the maximum correlation.

For this purpose, the detection matrix (DM) is formed as follows:

$$D_i = \begin{bmatrix} e^{-j\theta_i} & e^{j\theta_i} \end{bmatrix} \tag{4.12}$$

where θ_i is the delay associated with the angle of arrival (AOA) φ_i, as in (4.3). The analytical representation of the received signal compensates for the virtual delay θ_v at the output of the combiner, for two signals arriving from directions φ_{x1} and φ_{x2}, as in Figure 4.1. This is given by:

$$\mathbf{R} = \begin{bmatrix} e^{-j\theta_v} & e^{j\theta_v} \end{bmatrix} \begin{bmatrix} e^{j\theta_{x1}} & e^{j\theta_{x2}} \\ e^{-j\theta_{x1}} & e^{-j\theta_{x2}} \end{bmatrix} \begin{bmatrix} S(t) \\ S(t) \end{bmatrix} \tag{4.13}$$

Where the only one element of $\mathbf{R}$ is as follows:

$$\begin{aligned} R(t) &= S(t)\left(e^{j(\theta_{x1}-\theta_v)} + e^{-j(\theta_{x1}-\theta_v)}\right) \\ &+ S(t)\left(e^{j(\theta_{x2}-\theta_v)} + e^{-j(\theta_{x2}-\theta_v)}\right) \end{aligned} \tag{4.14}$$

Figure 4.4 shows the compensated received signal level R given in (4.14) versus the virtual angle of arrival, φ_v. This graph corroborates the result of (4.11), since it shows the appropriate compensation delay at the MCR for a combination of two signals arriving from two separate AOAs. According to (4.11), the compensation angle for two signals arriving from directions φ_{x1} and φ_{x2} is φ_v, a virtual angle of arrival that is associated with virtual delay θ_v, as calculated in (4.10). For this verification,
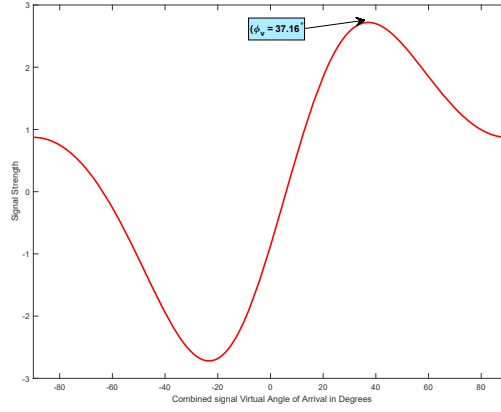
Figure 4.4: Combined signal with virtual AOA detection.

it is assumed that:

$\varphi_{x1} = 60°$ and $\varphi_{x2} = 20°$. As expected, peak shown in the graph occurs at $\varphi_v = 37.16°$, which is the same as predicted by using (4.11).

In the detection process, the TWO AOAs φ_{x1} and φ_{x2} are unknown; however, all the possible combinations of AOAs are known from the training phase. For the case analyzed, these combinations are given in Table 4.1. At the receiver, (4.14) is calculated for all valid combinations of AOAs, with the compensations related to the corresponding AOAs. This results in a maximum received signal level R, which is the received signal level compensated with the virtual angle of arrival $(AOA)_v$. Then from Table 4.1, the individual $(AOA)_v$ can be obtained.

Figure 4.5 provides a 3D graph representing (4.14), i.e., the signal strength during scanning for the combination of AOAs for signals arriving from two directions θ_{x1} and θ_{x2}. The graph shows that the compensated received signal peak for φ_v occurs at the correct AOAs: $\varphi_{x1} = 60°$ and $\varphi_{x2} = 20°$.
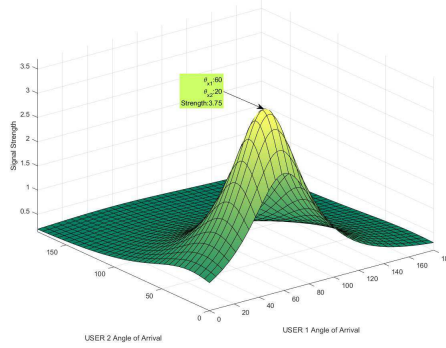
Figure 4.5: Optimization for signal detection.

4.2.5   Symbol Error Rate in AWGN

For M-ary signaling using ML detection in AWGN channels, the SER can be tightly upper bounded by:

$$SER \simeq \frac{M_{min}}{2}\text{erfc}\left(\sqrt{\frac{d_{min}^2}{4N_0}}\right) \tag{4.15}$$

where $\text{erfc}(\cdot)$ is the standard error function complement, d_{min} is the minimum Euclidian distance between the constellation points (signals in the absence of AWGN) at the receiver, N_0 is the noise power spectral density (PSD), and M_{min} is the number of points in the constellation reached with the minimum distance from the perspective of any point that results in a maximum of these numbers.

For a system with two users and two elements antenna array , the symbol inter-distances are:

$$d(\theta_{ij}, \theta_{lm}) =|\cos(\theta_i) + \cos(\theta_j)| - |\cos(\theta_l) + \cos(\theta_m)| \tag{4.16}$$

where θ_{xy} is the virtual delay related to angle of arrival φ_x and φ_y.

For a system with two users and four elements antenna array , the symbol inter-distances are given by 4.17:

$$d(\theta_{ij}, \theta_{lm}) = \mid \cos(\theta_i) + \cos(\theta_j) + \cos(3\theta_i) + \cos(3\theta_j) \mid$$
$$- \mid \cos(\theta_l) + \cos(\theta_m) + \cos(3\theta_l) + \cos(3\theta_m) \mid \tag{4.17}$$

4.2.6 Optimization

In the proposed system, at the link startup there is a training and optimization phase. By utilizing an optimization algorithm, the transmitter and the receivers determine the optimized beam angles for the targeted BER performance.

4.2.7 Interference Effects in Multi-Beam Systems

While the transmitter and receiver use a generic algorithm to optimize system performance, the energy associated with an individual user has an effect on other users, depending on the communication channel and beam widths. Increasing the number of users degrades the overall system performance. To minimize adjacent user beam interference, different antenna array topologies that are more resilient to adjacent beam interference can be used, e.g., a circular array.

Antenna polarization properties can also be used to improve the BER. Multi-polarized multi-beam arrays can provide a solution to reduce adjacent user interference. Specifically, signals with different polarization can reduce interference effects, even if the signals have the same AOA. Thus, the use of multi-polarization antenna arrays can significantly improve system performance.

4.3   Simulation Results

In this section, the performance of the BAMA scheme in a MIMO channel environment with various system parameters, in AWGN channel conditions, is evaluated by using Matlab simulations. The results are then compared with the analytical results presented in the previous section. Systems with two users are considered, where the number of beams or modulation levels $M_i = 2$, and the number of antenna array elements is set to 2, 4 and 8.

In the simulations, use of the ML receiver results in the same SER performance as in the case of the MCR. Based on (4.6), in BAMA, the SER or system performance depends upon the number of antenna and the radiation pattern used in the system. Increasing the number of antennas (diversity order) and decreasing the number of radiation patterns (modulation level) reduces the SER for a given SNR in a manner comparable to the situation with conventional amplitude and phase modulations. The SER results for binary signaling with $N_r = 2$, $N_r = 4$ and $N_r = 8$ in AWGN are presented. In the BAMA system, AOA optimization to reduce the SER can be performed in the transceiver training phase during the initial system startup, or when the system is re-initialized due to the changes in channel conditions, e.g., reflector positions. To evaluate the SERs in different scenarios, both optimized and non-optimized AOAs were used.

Figure 4.6 shows the SER for an AWGN channel for BAMA systems of two, four and eight antenna array elements, for non-optimized AOAs.

In Figure 4.7, which shows SER results with optimized angles, it can be observed that simple optimization yields 3dB performance improvement. The use of more sophisticated optimization determined by real-time and system complexity constraints can result in higher performance gains. In addition, the use of more complex AOA estimation approaches such as MUSIC and multiple snapshots could increase the
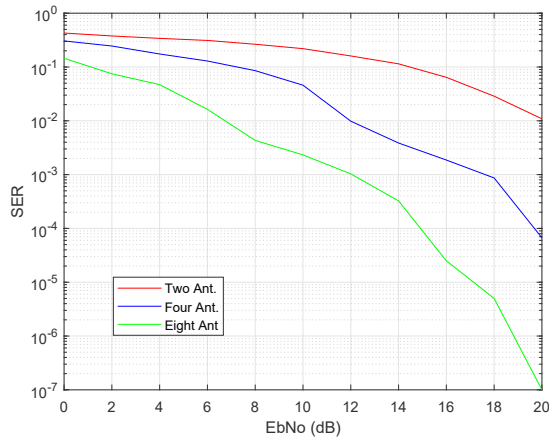
Figure 4.6: SER versus E_b/N_0, for non-optimized AOAs.

system performance. This needs to be further investigated in the future.
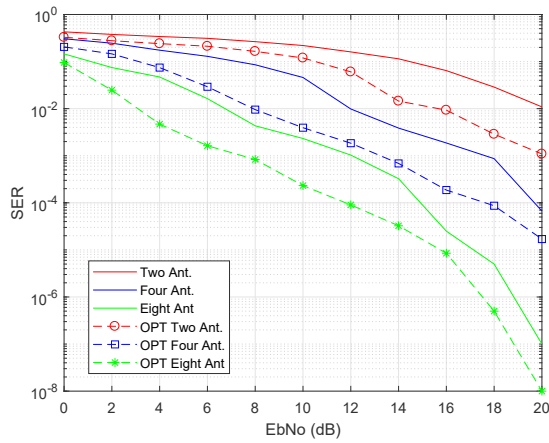
Figure 4.7: SER versus E_b/N_0, for optimized and non-optimized AOAs.

4.4   Summary

A multiple beam multiple access scheme on the uplink, referred to as beam angle multiple access (BAMA), has been developed in this chapter. The proposed scheme employs information-guided channel hopping [55] and represents an extension of the

beam angle shift keying (BASK) transmission technique to a multiuser scenario. BAMA works with a limited number of antennas for beamforming at the transmitters and the receiver. To compensate for BER performance losses, BAMA can employ a more advanced array signal processing strategy such as multiple snapshots for DOA detection.

5 Space-Time Block Coding Based on Antenna Radiation Pattern Switching

This chapter extends BACM with an antenna array to encode spatial symbols in the multiple angles of wave propagation (and arrival) in a wireless channel. In the case of two simultaneous beams, at the encoder, a block of information bits is mapped into three symbols: (i) one spatial symbol indexing two beams, representing the directions of departure (and hence arrival) of two amplitude- and phase-modulated (APM) carrier signals, and (ii) two APM symbols chosen from constellation diagrams such as QAM or PSK and independently transmitted over the two beams. Utilizing simultaneous transmissions on two (or multiple) beams improves the bandwidth efficiency as compared to that of the original BACM and is also used to benefit the diversity of the proposed system. Specifically, in the second part of this chapter, space-time block coding (STBC) strategies for generalized BACM are presented, which build on designs similar to STBC with generalized spatial modulation (G-SM). The performance of generalized BACM (G-BACM) with and without STBC is analyzed for multipath fading channels when trading off between the system data rate and reliability.

The chapter is organized into four sections. Section 5.1 gives a detailed description of the G-BACM system design. Section 5.2 then presents a proposed multi-beam block code transceiver. Sections 5.3 and 5.4 present the simulation results and chapter summary, respectively.

5.1   Generalized BACM Communication System

During a single channel use, G-BACM enables K active beams from a total of N_B potential beams generated in the transmit antenna array to send K APM symbols in parallel from QAM/PSK signal constellations. Changing the beam pattern for every channel use permits a set of beam combinations to be utilized to index spatial constellation points. At the transmitter, the incoming bits are mapped into two types of concatenated symbol: (i) one spatial symbol S_{BP}, which selects K active beams, i.e., a beam pattern, and which is identified with K indexes $(i_1, i_2 \cdots, i_K)$ where $i_1 < i_2 < \cdots < i_K \in \{1, 2, \cdots, B_K\}$) corresponding to the angles of departure (AOD) $(\Theta_{i_1}, \Theta_{i_2} \cdots \Theta_{i_K})$ for the K beams, and (ii) a group of K APM symbols, $S_1, S_2, \cdots, S_K$, from the M-ary QAM/PSK constellation. For a single channel use, depending on S_{BP}, the APM symbols $S_1, S_2, \cdots, S_K$ are transmitted on beams (in the transmit/receive antenna array plane) with angles $(\Theta_{i_1}, \Theta_{i_2} \cdots \Theta_{i_K})$, respectively. To simplify the notation, it is assumed that $\Theta_1 < \Theta_2 < \cdots < \Theta_{B_K}$. In addition, the symbol rates for spatial and APM symbol streams are assumed to be the same, and the switching rate for beam patterns is defined so that the duration of channel use is the same as the duration of individual symbols. Along any transmission path, the transmitted signal exhibits the on-off characteristics of a QAM/PSK signal. Thus, the bandwidth of the transmitted signal in the passband is considered to be twice the symbol rate, i.e., the beam pattern switching rate or the individual QAM stream rate.

The number of possible active beam combinations is $\binom{N_B}{K}$. Assuming that one spatial symbol is S_{BP} transmitted over the channel use, the number of beam combinations (defining the modulation level M_s for the spatial symbols) that can be considered for transmission must be a power of two. Therefore, only $M_s = 2^{m_s}$ combinations can be used, where $m_s = \left\lfloor \log_2 \binom{N_B}{K} \right\rfloor$ is the number of bits encoded on the

spatial symbol and $\lfloor \cdot \rfloor$ is the floor operator.

Transmitter operation in the G-BACM system model over two channel uses is depicted in Figure 5.1 for the case where $K = 2$ and $N_B = 4$. On the first channel
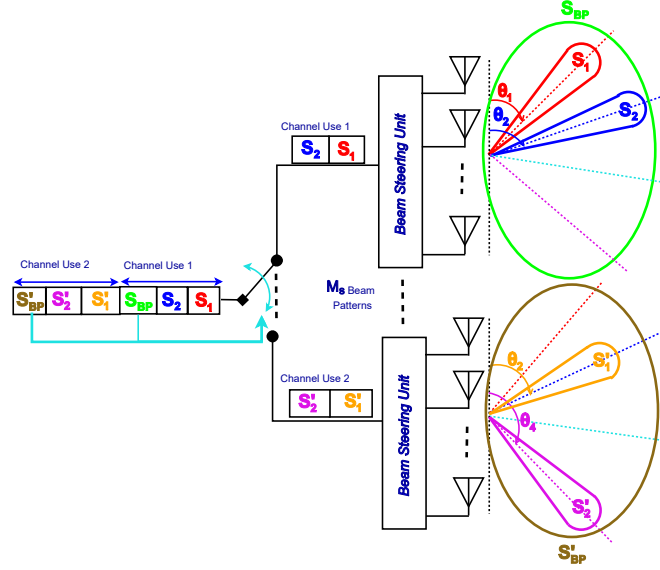
Figure 5.1: Generalized BACM transmitter operation over two channel uses.

use, the spatial symbol S_{BP} (from the possible $M_s = 4$) selects the upper branch, with two beams having angles Θ_1 and Θ_2 on which two QAM/PSK symbols S_1 and S_2 are sent, respectively. On the second channel use, the spatial symbol S'_{BP} selects the lower branch, with two beams having angles Θ_2 and Θ_4 on which again two QAM/PSK symbols S'_1 and S'_2 are sent. The use of branches in Figure 5.1 is for conceptual purposes only, since in a practical implementation the beam steering unit for all branches would be the same antenna array, with adaptive steering weights. Moreover, the actual number of transmit antennas N_t may be as low as two and is not related to N_B. The choice of N_t is determined by the beamforming gain requirement in the system.

In the system depicted in Figure 5.1, even though $\binom{N_B}{K} = 6$, the system works with $M_s = 4$, i.e., only four of six two-beam patterns are valid (for use as the actual

spatial symbols). Here, the modulation levels for spatial symbols in G-BACM and conventional BACM are the same. This is because in BACM only one beam is active for a single channel use and in the corresponding BACM system $\binom{N_B}{1} = 4$. The main difference in the bandwidth efficiency of G-BACM and BACM is that in G-BACM, $K = 2$ APM symbol streams are sent in parallel on K active beams, while in BACM only one APM symbol stream is sent. For a case with five possible beams ($N_B = 5$), where two beams are grouped, creating two APM symbol streams, the modulation level for spatial symbols in G-BACM would be $M_s = 2^{\lfloor \log_2 \binom{5}{2} \rfloor} = 8$, thus increasing the spectral efficiency for spatial symbols (as compared to BACM) from two bits per channel use to three bits per channel use.

5.1.1   Transmitter Operation in G-BACM

In conventional BACM, in order to transmit a QAM or PSK signal $s(t)$ in a single direction ($\Theta_k, \quad k = 1, \cdots, N_B)$) for the duration of one QAM/PSK symbol, the beamformer at the BACM transmitter feeds the ith ($i = 1, \cdots, N_t$) antenna array element with $s(t)$ weighted by $A_{i\Theta_k}$ to steer the beam in the single direction Θ_k [18]. Here, N_t is the number of antennas at the BACM transmitter. The beam steering vector mapper (BSVM) associated with each BACM spatial symbol/index defining one beam results in a distinct direction of departure (DOD) beam angle Θ_k. In conventional BACM, when transmitting one QAM or PSK modulated symbol, the beamformer selects one steering beam vector according to the spatial symbol/index from the DOD/DOA mapper.

One possible configuration for a G-BACM transmitter with beam patterns composed of $K = 2$ simultaneous beams would be $K = 2$ co-located antenna arrays, each implementing independent BACM as described in the preceding paragraph. The premise for this implementation is that G-BACM is essentially a superposition of individual BACMs. Specifically, the two APM symbol streams that should be sent

in G-BACM are fed after serial-to-parallel conversion in two BACM transmitters. The spatial symbol S_{BP} in G-BACM defining $K = 2$ outgoing beam angles $(\Theta_{i_1}, \Theta_{i_2})$ then defines individual beams with angles Θ_{i_1} and Θ_{i_2}, which are used in the BACM transmit antenna arrays with the corresponding BSVMs. The beam switching rate is the same in G-BACM and individual BACMs. The number of antennas in G-BACM would be $N_T = 2 \cdot N_t$. This implementation of G-BACM benefits from an over-the-air summation of two directional signals generated in two BACM antenna arrays.

In a case where the same APM data is transmitted on all active beams, i.e., with one APM symbol stream rather than K as presented here, the G-BACM could be considered as generalized SM, with multiple simultaneous active antennas with digital precoding/beamforming [56].

5.1.2 Receiver Operation in G-BACM

As in the previous sub-section, the focus is on systems using beam patterns composed of two beams with two APM symbol streams. This forms the basis for future generalizations. The receiver employs two phases. In the first phase, referred to as training, the G-BACM receiver uses an efficient DOA estimation/detection algorithm to determine the incoming signal beam pattern angles: $(\varphi_{k_1}$ and $\varphi_{k_2})$, $k_1, k_2 \in \{1, 2, 3, 4\}$, which also determines the spatial symbol $((S_{BP,k}, \quad k = 1, \cdots, M_s)$, i.e., one-to-one mapping between $(\varphi_{k_1}$ and $\varphi_{k_2})$ and $S_{BP,k}$. The next phase involves the actual data transmission, decoding QAM/PSK modulated signals and their angles of arrival (AOAs) $(\varphi_{k_1}$ and $\varphi_{k_2})$ (or rather their equivalents) determining the spatial symbol. For this phase, maximum likelihood (ML) decoding is used, as described below.

Without loss of generality, the receiver utilizes a uniform linear array (ULA) antenna with two elements $(N_r = 2)$, as shown in Figure 5.2. In order to detect the spatial symbol, the receiver should detect the AOAs, φ_1 and φ_2, (for two BACMs

forming a G-BACM) among the predetermined direction patterns that are designated for each symbol in the training phase of the initial link establishment.
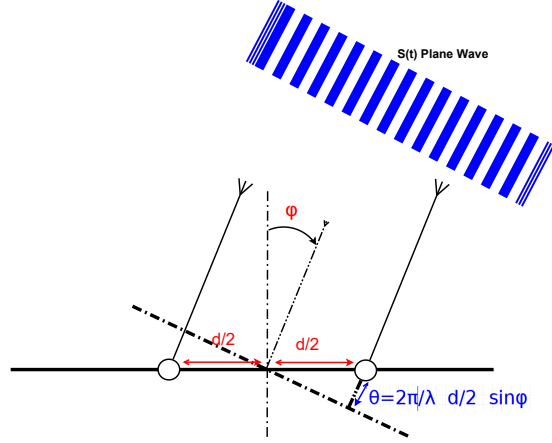
Figure 5.2: Uniform linear antenna array.

For a single plane wave $S(t)$ arriving from a single direction φ, the signal phase shift θ due to the delay at the left antenna element shown in Figure 5.2, referenced to the array center point, can be calculated as follows:

$$\theta = \frac{2\pi}{\lambda} \frac{d}{2} \sin \varphi \tag{5.1}$$

It is further assumed that $d = \lambda$. Therefore:

$$\theta = \pi \sin \varphi \tag{5.2}$$

When two QAM/PSK signals S_1 and S_2 from two BACM arrays arrive from unknown directions φ_{x1} from BACM array 1 and φ_{x2} from BACM array 2, the output of the antenna array, in the form of a vector, $\mathbf{R}$, is as follows:

$$\mathbf{R} = \begin{bmatrix} R_1 \\ R_2 \end{bmatrix} = \begin{bmatrix} e^{j\theta_{x1}} & e^{j\theta_{x2}} \\ e^{-j\theta_{x1}} & e^{-j\theta_{x2}} \end{bmatrix} \begin{bmatrix} S_1 \\ S_2 \end{bmatrix} + \begin{bmatrix} n_1 \\ n_2 \end{bmatrix} \tag{5.3}$$

where R_1 and R_2 represent baseband signals at individual antenna elements after matched filtering, and n_1 and n_2 stand for independent additive white Gaussian noise (AWGN) components at the corresponding antennas. If the receiver has an antenna array with N_r elements, the size of $\mathbf{R}$ is $N_r \times 1$. If there are K active beams defining spatial symbols, the size of a vector representing QAM/PSK symbols as in (5.3) would be $K \times 1$, and the 2×2 "rotation" matrix would be replaced by a matrix of size $N_r \times K$, defined by K phase shifts $\theta_{x1}, \cdots, \theta_{xK}$. The tacit assumption in (5.3) is that the signals arriving from different directions (along different paths) have the same power, with no fading. If this is not the case, it would be necessary to include multiplicative scaling factors in (5.3), which could be learned during the training phase or estimated based on the preamble signals. For example, if the average path gains in the channel for beams with phase shifts θ_{x1} and θ_{x2} were different and given by g_{x1} and g_{x2}, it would be necessary to scale S_1 and S_2 by g_{x1} and g_{x2}. In the rest of the dissertation, the path loss $g_{x1} = g_{x2} = 1$ is assumed for all beams.

ML decoding of the QAM/PSK symbols, S_1 and S_2, and the two angles of arrival (AOAs), φ_{x1} and φ_{x2}, based on (5.3), would require calculating in advance all possible "valid" codewords (or super-symbols):

$$\mathbf{SS}(x,p,q) = \begin{bmatrix} e^{j\theta_{x1}} & e^{j\theta_{x2}} \\ e^{-j\theta_{x1}} & e^{-j\theta_{x2}} \end{bmatrix} \begin{bmatrix} S_1(p) \\ S_2(q) \end{bmatrix} \tag{5.4}$$

for all combinations of QAM/PSK symbols (given by indexes $p, q \in \{1, \cdots, M\}$) and spatial symbols defined by AOAs φ_{x1} and φ_{x2}, or equivalently by phase shifts θ_{x1} and θ_{x2}, where $x \in \{1, \cdots M_s\}$. There are $M_s \cdot M^2$ valid codewords when $K = 2$.

For a fading environment with fading coefficients on beam xi ($i \in \{1, 2\}$) to the jth ($j \in \{1, 2\}$) receive antenna array element given by h_{ji}, the super-symbols in (5.4)

would be modified as follows:

$$\mathbf{SS}_{\text{fade}}(x,p,q) = \begin{bmatrix} h_{x11}e^{j\theta_{x1}} & h_{x12}e^{j\theta_{x2}} \\ h_{x21}e^{-j\theta_{x1}} & h_{x22}e^{-j\theta_{x2}} \end{bmatrix} \begin{bmatrix} S_1(p) \\ S_2(q) \end{bmatrix} \qquad (5.5)$$

In Rayleigh fading channels, h_{ji}s are complex normal random variables (RVs) with a variance of one and zero mean ($h_{ji} \sim \mathcal{CN}(0,1)$) and are usually independent of one another other. During decoding, for every received vector $\mathbf{R}$, the Euclidean distances between $\mathbf{R}$ and the valid codewords ($\mathbf{SS}(x,p,q)$ (or $\mathbf{SS}_{\text{fade}}(x,p,q)$)) are calculated. The ML principle of choosing the super-symbol is then applied, so as to minimize the distance when making the final decision. Here, a single decision determines the super-symbol, or rather the concatenated symbols S_1, S_2 and S_{BP}.

In some scenarios, like one presented in the following section, it may be desirable to decode/determine the spatial symbol or equivalently the angles of arrival for $K = 2$ beams independently of the transmitted S_1 and S_2 APM symbols, e.g., when S_1 and S_2 are already known. The objective here is to use simplified detection rather than ML. To this end, based on (5.3) and following the approach described in [19], a maximum correlation receiver (MCR) is developed that projects the received vector signal $\mathbf{R}$ onto all M_s "valid" vectors, conditioned on $\hat{S}_1$ and $\hat{S}_2$:

$$\mathbf{V}_{\hat{S}_1,\hat{S}_2}(x) = \begin{bmatrix} e^{j\theta_{x1}} & e^{j\theta_{x2}} \\ e^{-j\theta_{x1}} & e^{-j\theta_{x2}} \end{bmatrix} \begin{bmatrix} \hat{S}_1 \\ \hat{S}_2 \end{bmatrix} \quad x \in \{1, \cdots, M_s\} \qquad (5.6)$$

where $\hat{S}_1$ and $\hat{S}_2$ stand for the specific realization of generic APM symbols S_1 and S_2. The M_s valid vectors in (5.6) would have to be calculated for all possible pairs of phase shifts, θ_{x1} and θ_{x2}, defining M_s possible spatial symbols S_{BP}, i.e., arriving beam patterns. In (5.6), as in (5.4), if signals S_1 and S_2 arrive following random fading, knowing h_{xji} gains, it would be necessary to scale the "rotation" matrix in

(5.6), as was done when proceeding from (5.4) to (5.5). For already detected APM symbols, $\hat{S}_1$ and $\hat{S}_2$ for a given channel use, it would be necessary to calculate M_s inner products:

$$\Re\left(\mathbf{R}^H \cdot \mathbf{V}_{\hat{S}_1, \hat{S}_2}(x) \right) \tag{5.7}$$

where ^{H} is the Hermitian transpose and $\Re(\cdot)$ represents the real part. Finally, a decision is made on the index of the spatial symbol resulting in the maximum value among M_s decision variables calculated in (5.7).

The symbol error rate (SER) performance of the ML and MCR detectors depends upon the Euclidian distances between valid vectors, i.e., the inter-distances between $\mathbf{SS}(x, p, q)$ in ML, and the inter-distances between $\mathbf{V}_{\hat{S}_1, \hat{S}_2}(x)$ in MCR. Deciding upon the choice of AODs/AOAs to maximize the inter-distances (or equivalently to minimize the SER) for a given K and M may require involved optimization and is beyond the scope of this paper. The problem becomes even more complex when the fading environment is considered.

5.2   Multi-Beam Block Coded G-BACM Transceiver

In the proposed implementation of a multi-beam block coded G-BACM transceiver, conventional STBC is applied for the APM symbols, and the system benefits from repetition coding (diversity combining) for the spatial symbols. The principles involved are demonstrated for the case of groups of $K = 2$ beams, similarly to the approach used in the previous section for demonstrating the principles underlying the uncoded G-BACM.

Figure 5.3 illustrates the multi-beam block coded G-BACM concept. The Alamouti scheme is considered as an example due to its low decoding complexity and implementation simplicity. As in the case of orthogonal STBC-MIMO without adaptive beamforming, two PSK/QAM symbols (S_1 and S_2) are first encoded and then

simultaneously transmitted on a pair of selected beams in two channel uses. During these two channel uses, the same two beams are employed, i.e., the spatial symbol (indexing the pair of beams) is the same for two channel uses. Essentially, the encoder represented in Figure 5.3 processes the information symbols in blocks of three symbols over two channel uses, while in the uncoded G-BACM shown in Figure 5.1, there would be six symbols over two channel uses. In this way, the data rate of the proposed coded system is halved.
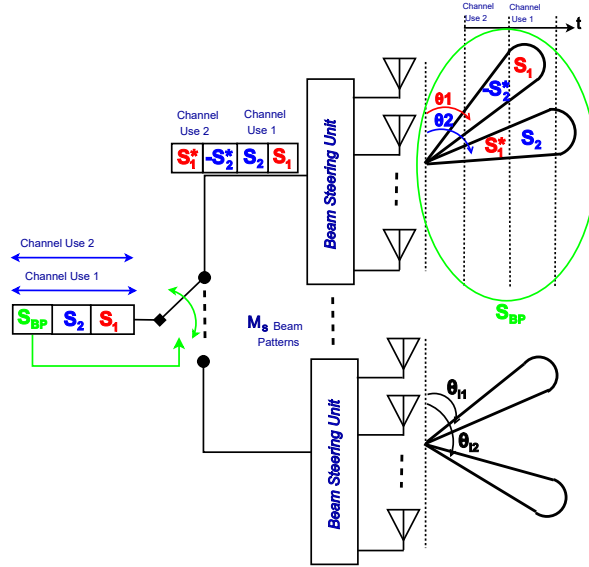
Figure 5.3: G-BACM with Alamouti scheme for APM symbols and diversity combining for spatial symbols.

In the original application of Alamouti STBC in MIMO channels, a complex symbol pair (S_1 and S_2) is transmitted orthogonally from two transmit antennas in two symbol intervals, with the codeword $\mathbf{S} = \begin{bmatrix} S_1 & -S_2^* \\ S_2 & S_1^* \end{bmatrix}$ where the rows and columns correspond to the transmit antennas and the symbol intervals, respectively. It is assumed that the channel gains between transmit and receive antennas remain constant for the two time slots. When a signal is received in a MIMO Rayleigh fading

channel using N_r receive antennas, with simple and efficient receiver processing, the Alamouti STBC diversity order for the two transmit antennas is $2 \cdot N_r$.

For the proposed multi-beam block coded G-BACM, Alamouti STBC is applied on two transmit beams to benefit from the transmit antenna gains. When two directional carrier signals arrive at the receiver they are superimposed at the antenna elements, as in the case of a MIMO channel with omnidirectional transmit antennas. Thus, receiving APM signals from two directions on N_r antennas over two channel uses requires implementation of the same maximum ratio combining processing as in OSTBC-MIMO. In STBC G-BACM this offers the same diversity of $2 \cdot N_r$, provided that the fading coefficients along each beam and for different antennas are independent RVs.

Once the APM symbols S_1 and S_2 are recovered by using maximum ratio combining for the 2×2 Alamouti scheme, the modified version of MCR described at the end of the previous section is used for the detection of the spatial symbol S_{BP}. In the proposed coded G-BACM scheme, because the same beam pair is employed in two consecutive channel uses, for each channel use decision variables are calculated, as in (5.7), for two receive vectors, $\mathbf{R}_{cu1}$ and $\mathbf{R}_{cu2}$, representing the signals received at the receive antenna array during the first and second channel use.

To minimize the effects of noise, for a given potential spatial symbol S_{BP} indexed by $x \in \{1, \cdots, M_s\}$, with corresponding phase shifts, the decision variables are averaged and the following calculation is performed:

$$D(x) = \Re\left(\left(\mathbf{R}_{cu1}^{H} \cdot \mathbf{V}_{\text{fade},\hat{S}_1,\hat{S}_2}(x) \right) + \left(\mathbf{R}_{cu2} \cdot \mathbf{V}_{\text{fade},-\hat{S}_2^*,\hat{S}_1^*}(x) \right) \right) \qquad (5.8)$$

where, in a fading environment:

$$\mathbf{V}_{\text{fade},\hat{S}_1,\hat{S}_2}(x) = \begin{bmatrix} h_{x11}e^{j\theta_{x1}} & h_{x12}e^{j\theta_{x2}} \\ h_{x21}e^{-j\theta_{x1}} & h_{x21}e^{-j\theta_{x2}} \end{bmatrix} \begin{bmatrix} \hat{S}_1 \\ \hat{S}_2 \end{bmatrix} \qquad (5.9)$$

The index x of the spatial symbol resulting in the maximum value among M_s decision variables $D(x)$, calculated in (5.8), would determine the actually encoded spatial symbol, i.e., the beam pattern given by θ_{x1} and θ_{x2}.

5.3   Simulation Results and Analysis

This section presents simulation results for G-BACM with and without the proposed use of STBC in Rayleigh fading environments. The bit error rate (BER) performance of these systems was evaluated by using Monte Carlo simulations for various numbers of receive antennas, as a function of the average SNR per receive antenna. For the simulations, in all cases it was assumed (i) that $N_B = 4$ and $K = 2$, resulting in $M_s = 4$ beam patterns, and (ii) that QPSK signaling on APM symbols was used. The coded systems operate with throughput reduced by half. Figures 5.4 and 5.5 show the BER curves for the G-BCAM system with and without STBC,
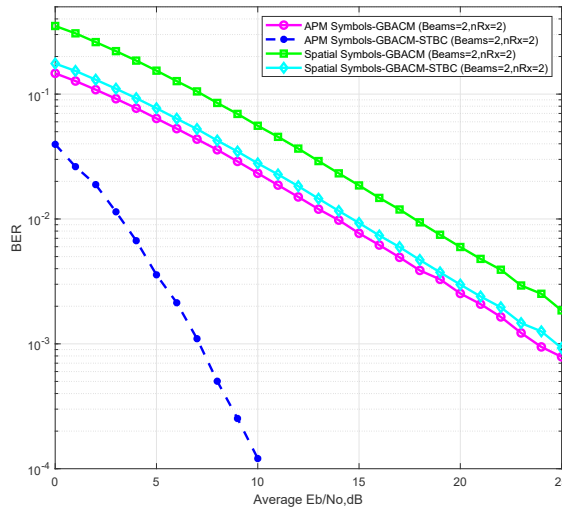

Figure 5.4: G-BACM BER performance for spatial and QPSK symbols in a Rayleigh fading environment, with and without STBC, for $K = 2$ and $N_r = 2$.

when $N_r = 2$ and $N_r = 4$, respectively. The AOAs for $N_B = 4$ possible beams were adjusted to: $\varphi_1 = 95°$, $\varphi_2 = 45°$, $\varphi_3 = -45°$ and $\varphi_4 = -90°$ in both systems, with $N_r = 2$ and $N_r = 4$ receive antennas. $M_s = 4$ pairs of these angles were used, except for two pairs: (φ_1, φ_2) and (φ_2, φ_3). It was verified that these AOA choices and corresponding beam patterns achieve good separation between the decision variables in (5.7) when MCR is used to detect the spatial symbols.
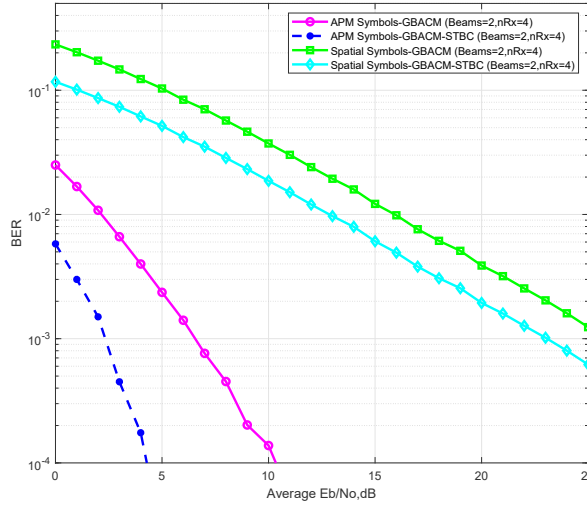
Figure 5.5: G-BACM BER performance for spatial and QPSK symbols in a Rayleigh fading environment, with and without STBC, for $K = 2$ and $N_r = 4$.

From the results shown in Figures 5.4 and 5.5, it can be seen that the number of receive antennas improves BER performance significantly for both spatial and APM bit streams. The slopes of the G-BACM BER curves for APM symbols S_1 and S_2, with the Alamouti coding scheme, indicate diversity gain in the order of $2 \cdot 2$ and $2 \cdot 4$ for $N_r = 2$ and $N_r = 4$, respectively. This is in agreement with the discussions in the previous section. For a BER value of 10^{-3}, the coding gain of G-BACM with the Alamouti scheme for APM bits is 17dB and 4dB in comparison to G-BACM with ML decoding, for systems with $N_r = 2$ and $N_r = 4$ receive antennas, as shown in Figures 5.4 and 5.5.

The BER curves for spatial symbols encoded in beam patterns exhibit "linear" behavior (on the log-log scale), indicating that here the system benefits from diversity effects. This is partially due to the fact that repetition coding and equal gain combining are used for decision variables when differentiating between spatial symbols using MCR. There is unbalanced BER performance for the spatial and APM data streams, which may require more sophisticated optimization of AOAs or the use of different coding strategies. For a BER value of 10^{-3}, the coding gain of G-BACM with repetition coding on spatial bits in comparison to G-BACM with ML decoding of the superposed symbols (S_1, S_2, S_{BP}) is around 3dB in both systems, with $N_r = 2$ and $N_r = 4$ receive antennas, as shown in Figures 5.4 and 5.5.

In addition to the performance trade-offs between multiplexing and diversity gains in coded and uncoded G-BACM, it should be noted that the coded system with decoding over two channel uses allows decoupling of the detection of APM symbols and spatial symbols. This results in lower complexity detection in G-BACM with STBC, as compared to ML decoding in uncoded G-BACM. Moreover, the BER versus received SNR curves do not account for the transmit antenna gain, which is the most important benefit of this scheme.

While increasing bandwidth efficiency and reliability and, to a certain extent, minimizing interference as in space division multiple access (SDMA), the G-BACM scheme is an attempt to take advantage of large (adaptive) antenna arrays that can be packed compactly at both the transmitter and the receiver, due to decreased wavelengths in future wireless systems operating at higher frequencies. Another feature of the proposed G-BACM is that by utilizing data-driven (random) beam patterns, the scheme has the potential to be used in physical layer security solutions.

5.4 Summary

A multiple beam extension of beam angle channel modulation (BACM), referred to as generalized BACM (G-BACM), has been presented in this chapter. The proposed scheme yields improved bandwidth efficiency in comparison to the original BACM by enabling simultaneous QAM/PSK stream transmissions on multiple beams, as well as indexing the transmission beams with spatial symbols. More importantly, like BACM, G-BACM benefits from antenna beamforming gains. To compensate for BER performance losses in fading channels, in the second part of this chapter G-BACM was configured to benefit from the transmit diversity gain of STBC and repetition coding on APM and spatial symbols, respectively. In conclusion, G-BACM with and without STBC could be a useful signaling technique in future mmWave communication systems, where MIMO digital beamforming is essential to combat high signal attenuation.

6   Conclusions and Future Work

This dissertation has developed new techniques to improve spectral efficiency in digital communication systems, by employing smart antenna arrays to encode data at the RF level. The most important aspect of all the proposed schemes is that they benefit from antenna gains. Specifically, in these systems, at the transmitter, the spatial symbols are mapped into the beam angle index of the radiated pattern; and at the receiver, the spatial symbols are recovered through the detection of the AOA(s) and the corresponding spatial symbol index. The bandwidth improvement is the result of concatenating the new modulation scheme with regular amplitude and phase modulation to create a dual layer modulation. Furthermore, based on this technique, new space-time block coding to improve reliability, and multiple access schemes to accommodate multi-user transmissions have been introduced. Working with beamforming patterns offers the benefit of realizing high modulation levels for spatial symbols, with a relatively small number of antennas. This contrasts with similar index modulation schemes such as SM, where the spatial modulation level is the same as the number of antennas. Moreover, the beamforming approach provides flexibility by selecting the communication channels to achieve optimized performance. Adaptive beamforming pattern selection offers an advantage over SM, where communication channels are dictated by the spatial location of the antennas, which means that SM does not have link optimization capability. The method proposed here also reduces the number of RF chains. The performance of the developed schemes was simulated and optimized

for different propagation environments, with different antenna configurations. The specific contributions of the dissertation are reviewed in Section 6.1 and potential further research is suggested in Section 6.2.

6.1   Dissertation Contributions and Summary

The following are the specific contributions of this work:

1. Beamforming was used to encode data in the beam angle of the power radiated in the wireless channel, leading to the development of beam angle shift keying (BASK) modulation.

   At the RF stage, BASK employs an antenna array to encode information bits in the angle of the transmitting beam. Specifically, the one-dimensional (1D) indices representing data symbols directly modify the radiation characteristics of the transmitting antenna array via the spatial symbol rate, when sending an unmodulated carrier signal (without APM). Through specular reflection paths, the carrier signal is assumed to arrive at the receiver from one direction for the duration of the spatial symbol. At the receiver, a maximum likelihood (ML) detector differentiates between the direction of arrival from different beams indexing spatial symbols. Beamforming and activation of one of the beams at the transmitter can be accomplished by using adaptive antenna arrays. Beams resulting in optimum system performance are determined during the training phase. Moreover, the proposed schemes inherit all the advantages of a smart antenna system that are described in Section 1.3.1: specifically, higher gain, higher throughput, and multipath mitigation.

2. The proposed BASK technique was further extended to develop a concatenated 3D modulation scheme referred to as beam angle channel modulation (BACM). In

addition to encoding the information bits in the angle of the transmitting beam, BACM also includes conventional 2D QAM or PSK on the same RF carrier. At the encoder, the block of information bits is mapped into two symbols: (i) a spatial symbol selecting the direction of departure, and consequently the direction of arrival, of the amplitude and phase modulated carrier signal, and (ii) a temporal symbol chosen from the constellation diagram, such as QAM or PSK. Use of the transmitted signal angle through antenna array beamforming increases the spectral efficiency of single-input single-output (SISO) conventional (temporal) modulation by the base-two logarithm of the number of spatial beams that can be resolved (detected) at the receiver.

3. The BASK modulation scheme was employed in a multi-user scenario on the uplink, which resulted in the development of an interference-aware multi-user detection technique referred to as beam angle multiple access (BAMA). In the system, multiple access is achieved by assigning subsets of beams to individual users signaling with BASK. At the base station, for the duration of the spatial symbol, the receiver decides on a subset of possible multiple angles of arrival (AOA), corresponding to synchronized spatial symbols from different users. Unlike the situation in spatial division multiple access, where a fixed beam arrangement is used, BAMA detects the beams used by multiple users on a symbol-by-symbol basis.

4. Furthermore, generalized BACM (G-BACM) was introduced to allow the spatial symbol at the transmitter to select a beam pattern with two or more active beams. In generalized BACM, for a single channel use, the transmitted information is conveyed (i) in spatial symbols indexing the activated combination of multiple (two or more) simultaneous transmit/receive beams, and (ii) in multiple APM symbols from QAM/PSK constellations. All the APM symbol streams

are transmitted in parallel on the active beams. Working with combinations of multiple active beams (of the total number of potential beams generated in the transmit antenna array) increases the spatial modulation level in G-BACM, in comparison to that in the original BACM.

5. The concept of G-BACM was combined with space-time block coding (STBC) strategies to improve the spatial symbol detection reliability. In this dissertation, the Alamouti code for the APM symbols was the STBC technique applied, to take advantage of the multiplexing gain in G-BACM to improve system reliability. In the implementation of STBC, reusing the same group of two beams in two consecutive channel uses reduces the spatial symbol rate, in a trade-off between the system error rate and system throughput. Having two versions of the transmitted symbol for decision variables when deciding on the spatial symbols also improves the spatial symbol error rate.

6.2   Suggested Future Work

Several topics for future research are suggested in this section. Some of these issues, such as the need for practical verification, are inherent in all theoretical investigations of signal processing algorithms, while others are specific to the schemes proposed here.

1. Design and development of a hardware BACM-based communication platform.

   The research in this dissertation was performed at an analytical level and verified with simulations. The focus is on algorithmic development for the transceiver, and theoretical performance evaluation. Most of the schemes developed in this work build on the assumption of the existence of specular reflection paths, where a signal transmitted in one direction results in a single angle of arrival of the

received radio frequency (RF) wave. To confirm the simulation results and to check the practicality of the assumptions, a hardware platform for a transceiver with dynamically adjusted radiation patterns needs to be designed and built. Such a system should include a DSP module to generate and synchronize the smart antenna feed signals, and could include a FPGA module for fast switching of the antenna feeds at the transmitter and receiver. Hardware-software co-design methodology could permit verification of the proposed communication system synthesized first in the simulation environment, and then tested on a real-world transceiver with real-world MIMO channels.

2. Investigation of the effect of differences in the antenna array structure, polarization and signal power.

Adaptive antennas, with the gain and phase of signals induced in various antenna elements adjusted as required by transceivers, play a major role in the performance of the proposed system. While achieving a directional radiation pattern with high directivity and low side lobe levels is tacitly assumed in this dissertation, the receiver antenna array and corresponding performance evaluation are always based on a LUA assumption. LUAs occupy a unique position in array theory and are a major focus of attention. This is a reason why they have been used in the present analysis, to gain valuable insights into the performance of the proposed signaling schemes. However, antenna arrays can assume any geometric form. Various array geometries which are commonly of interest are: nonuniform linear arrays, circular arrays, planar arrays, and conformal arrays. The investigation of the performance of the proposed systems with different antenna array geometries is a requirement for designing high-performance communication systems based on BACM.

Here it has also been assumed that all incident signals arriving via all directions and specular reflection paths have equal power magnitudes, which may not always be realistic. Therefore, the effects of differences in signal power (and polarization) on AOA detection should be considered.

3. Investigation of the use of more advanced optimization techniques for AOAs.

Optimization methods are essential in the design of communications and signal processing algorithms. An important challenge for the proposed systems is to find optimized AOAs during the training phase, to achieve improved AOA detection. The simulations employed in the present research utilize a generic exhaustive search algorithm that is useful for many ill-structured global optimization problems with discrete and continuous variables. However, the algorithm involves high computational complexity, and may be impractical in real-time implementations. Therefore, it would be of interest to determine if the optimization problems in this work could be cast in the form of convex optimization problems, where the structure of the optimal solution often provides design insights. If implementation of the structured optimization methods proves prohibitively complex, metaheuristic search algorithms could be pursued, such as genetic algorithms, tabu search, simulated annealing, evolutionary programming, ant colony optimization, particle swarm optimization, cross-entropy, multistate, clustering algorithms, or stochastic approximation. Finding a more efficient AOA optimization method that results in a lower symbol error rate (SER) and faster training times would significantly improve the performance of the proposed system.

4. The use of pseudospectrum estimation for AOA detection.

The objective of angle of arrival (AOA) detection based on AOA estimation techniques is to specify a function of the AOA, traditionally referred to as

pseudospectrum $P(\theta)$, that provides a maximum output in the direction of the received signal. In addition to the linear post-processing pursued in this dissertation, there are several other potential approaches for obtaining a pseudospectrum through beamforming, including: an array correlation matrix, eigenanalysis, linear prediction, minimum variance, maximum likelihood, minnorm, MUSIC, and root-MUSIC, which could be evaluated in the context of this research. Each of these techniques has advantages and disadvantages. A detailed investigation is required, first to set comparison criteria such as the bandwidth and number of antenna arrays, and then to differentiate and prioritize the methods with regard to the application presented here.

5. Improving the performance of a communication system by using directional switching.

This dissertation employs the radiation beam angle as a data encoding parameter. An alternate use of beam switching is to create multiple channels between the transmitter and the receiver. For instance, a system with four beams has one main channel and three reserved channels. Such a system can switch between the main channel and reserved channels to optimize communication link performance in terms of diversity gain. In this case, the beam index does not convey any spatial information. This application of smart antenna beam switching can be a seed for future research.

Bibliography

[1] C. Lim, T. Yoo, B. Clerckx, B. Lee, and B. Shim, "Recent trend of multiuser MIMO in LTE-advanced," *IEEE Trans.Commun. Mag.*, vol. 51, no. 3, pp. 127–135, 2013.

[2] A. Sibille, C. Oestges, and A. Zanella, *MIMO: From Theory to Implementation.* Academic Press, 2010.

[3] D. Bliss, K. Forsythe, and A. Chan, "MIMO wireless communication," *Linconlan Laboratory Journal*, vol. 15, no. 1, pp. 97–126, 2005.

[4] A. Goldsmith, *Wireless Communications.* Cambridge University Press, 2005.

[5] M. Jankiraman, *Space-Time Codes and MIMO Systems*, ser. The Artech house universal personal communications series. Artech House, Incorporated, 2004.

[6] D. Tse and P. Viswanath, *Fundamentals of Wireless Communication.* New York, NY, USA: Cambridge University Press, 2005.

[7] L. C. Godara, "Applications of antenna arrays to mobile communications. i. performance improvement, feasibility, and system considerations," *Proc. IEEE*, vol. 85, no. 7, pp. 1031–1060, July 1997.

[8] P. S. Jian Li, *Robust Adaptive Beamforming*, 3rd ed. Upper Saddle River, NJ, USA: John Wiley & Sons, Inc., 2005.

[9] A. Kanatas, K. Nikita, and P. Mathiopoulos, *New Directions in Wireless Communications Systems: From Mobile to 5G.* CRC Press LLC, 2017.

[10] Y. Huang, Y. Li, H. Ren, J. Lu, and W. Zhang, "Multi-panel MIMO in 5G," *IEEE Trans.Commun. Mag.*, vol. 56, no. 3, pp. 56–61, MARCH 2018.

[11] Y. Ding, K. J. Kim, T. Koike-Akino, M. Pajovic, P. Wang, and P. Orlik, "Spatial scattering modulation for uplink millimeter-wave systems," *IEEE Communications Letters*, vol. 21, no. 7, pp. 1493–1496, July 2017.

[12] X. Tan, Z. Sun, D. Koutsonikolas, and J. M. Jornet, "Enabling indoor mobile millimeter-wave networks based on smart reflect-arrays," in *IEEE INFOCOM 2018 - IEEE Conference on Computer Communications*, April 2018, pp. 270–278.

[13] L. C. Godara, "Application of antenna arrays to mobile communications. ii. beam-forming and direction-of-arrival considerations," *Proc. IEEE*, vol. 85, no. 8, pp. 1195–1245, Aug 1997.

[14] N. Ishikawa, S. Sugiura, and L. Hanzo, "50 years of permutation, spatial and index modulation: From classic rf to visible light communications and data storage," *IEEE Communications Surveys Tutorials*, vol. 20, no. 3, thirdquarter 2018.

[15] F. Xiong, *Digital Modulation Techniques*, ser. Artech House telecommunications library. Artech House, 2000.

[16] E. Lee and D. Messerschmitt, *Digital Communications*. Kluwer Academic Publishers, 1992.

[17] J. Hoseyni and J. Ilow, "M-ary beam angle shift keying modulation for MIMO channels," in *2018 Wireless Days (WD)*, April 2018, pp. 190–195.

[18] J. Hoseyni and J. Ilow, "Beam angle channel modulation," in *2017 IEEE 86th Vehicular Technol. Conf. (VTC-Fall)*, Sept 2017, pp. 1–6.

[19] J. Hoseyni and J. Ilow, "A novel multiple access technique based on antenna radiation pattern modulation," in *2018 IEEE 29th Annual International Symposium on Personal, Indoor, and Mobile Radio Communications (PIMRC)*, Sept 2018, pp. 1–6.

[20] J. Hoseyni and J. Ilow, "Generalized beam angle channel modulation with space-time block coding," in *2019 IEEE 90th Vehicular Technol. Conf. (VTC-Fall)*, Sept 2019, pp. 1–6.

[21] F. R. P. Cavalcanti and S. Andersson, Eds., *Optimizing Wireless Communication Systems*. Springer Publishing, 2009.

[22] W. Stallings, *Data And Computer Communications*. Pearson/Prentice Hall, 2007.

[23] M. Wen, X. Cheng, and L. Yang, "Optimizing the energy efficiency of ofdm with index modulation," in *2014 IEEE International Conference on Communication Systems*, Nov 2014, pp. 31–35.

[24] E. Basar, "Index modulation techniques for 5G wireless networks," *IEEE Communications Magazine*, vol. 54, no. 7, pp. 168–175, July 2016.

[25] A. K. Khandani, "Media-based modulation: A new approach to wireless transmission," in *2013 IEEE International Symposium on Information Theory*, July 2013, pp. 3050–3054.

[26] J. Mietzner, R. Schober, L. Lampe, W. H. Gerstacker, and P. A. Hoeher, "Multiple-antenna techniques for wireless communications - a comprehensive literature survey," *IEEE Communications Surveys Tutorials*, vol. 11, no. 2, pp. 87–105, Second 2009.

[27] J. Jeganathan, A. Ghrayeb, L. Szczecinski, and A. Ceron, "Space shift keying modulation for MIMO channels," *m-ieee-wireless-trans*, vol. 8, no. 7, pp. 3692–3703, July 2009.

[28] W. Popoola, E. Poves, and H. Haas, "Generalised space shift keying for visible light communications," in *2012 8th International Symposium on Communication Systems, Networks Digital Signal Processing (CSNDSP)*, July 2012, pp. 1–4.

[29] R. Y. Mesleh, H. Haas, S. Sinanovic, C. W. Ahn, and S. Yun, "Spatial modulation," *IEEE Transactions on Vehicular Technology*, vol. 57, no. 4, pp. 2228–2241, July 2008.

[30] P. Yang, M. Di Renzo, Y. Xiao, S. Li, and L. Hanzo, "Design guidelines for spatial modulation," *IEEE Communications Surveys Tutorials*, vol. 17, no. 1, pp. 6–26, Firstquarter 2015.

[31] M. D. Renzo, H. Haas, and P. M. Grant, "Spatial modulation for multiple-antenna wireless systems: a survey," *IEEE Communications Magazine*, vol. 49, no. 12, pp. 182–191, December 2011.

[32] J. Proakis, *Digital communications*. McGraw-Hill, New York, 2015.

[33] M. D. Renzo, H. Haas, A. Ghrayeb, S. Sugiura, and L. Hanzo, "Spatial modulation for generalized MIMO: Challenges, opportunities, and implementation," *Proceedings of the IEEE*, vol. 102, no. 1, pp. 56–103, Jan 2014.

[34] J. Jeganathan, A. Ghrayeb, L. Szczecinski, and A. Ceron, "Space shift keying modulation for mimo channels," *IEEE Transactions on Wireless Communications*, vol. 8, no. 7, pp. 3692–3703, July 2009.

[35] R. Mesleh and A. Alhassi, *Space Modulation Transmission and Reception Techniques*. Wiley, 2018, pp. 35–83. [Online]. Available: https://ieeexplore.ieee.org/document/8368001

[36] L. Lampe, A. M. Tonello, and T. G. Swart, *Digital Transmission Techniques*. Wiley, 2014. [Online]. Available: https://ieeexplore.ieee.org/document/8043331

[37] R. Y. Mesleh, H. Haas, S. Sinanovic, C. W. Ahn, and S. Yun, "Spatial modulation," *IEEE Transactions on Vehicular Technology*, vol. 57, no. 4, pp. 2228–2241, July 2008.

[38] K. V. Nair and P. R. Prabhu, "A comparative study on multiple active spatial modulation in mimo systems," in *2014 International Conference on Control, Instrumentation, Communication and Computational Technologies (ICCICCT)*, July 2014, pp. 457–460.

[39] S. Wang, W. Li, and J. Lei, "Physical-layer encryption in massive mimo systems with spatial modulation," *China Communications*, vol. 15, no. 10, pp. 159–171, Oct 2018.

[40] S. S. Pillai, S. Dhanya, and B. K. Jeemon, "Performance comparison of multicast mimo systems employing spatial modulation and coded spatial modulation in fading channels," in *2017 International Conference on Intelligent Computing, Instrumentation and Control Technologies (ICICICT)*, July 2017, pp. 1529–1533.

[41] W. Gao, *Energy and Bandwidth-Efficient Wireless Transmission*. Springe, 2017.

[42] R. Horak, *Telecommunications and Data Communications Handbook*. New York, NY, USA: John Wiley & Sons, Inc., 2007.

[43] J.-C. Bic, *Radio Wave Propagation for Telecommunication Applications*. Springe, 2005.

[44] J. Paulraj, *MIMO Wireless Communications*. San Diego, California, USA: Academic Press, 2007.

[45] K. Sundaravadivu and S. Bharathi, "Stbc codes for generalized spatial modulation in mimo systems," in *2013 IEEE International Conference ON Emerging Trends in Computing, Communication and Nanotechnology (ICECCN)*, March 2013, pp. 486–490.

[46] S. M. Alamouti, "A simple transmit diversity technique for wireless communications," *IEEE Journal on Selected Areas in Communications*, vol. 16, no. 8, pp. 1451–1458, Oct 1998.

[47] C. A. Balanis, *Antenna Theory: Analysis and Design*. Wiley-Interscience, 2005.

[48] R. Janaswamy, *Radio Wave Propagation and Smart Antennas for Wireless Communications*. Kluwer Academic Publishers, 2002.

[49] S. Drabowitch, *Modern Antennas*. Springer, 2005.

[50] R. L. Haupt, *Antenna Engineering Handbook, Fifth Edition*. New York, NY, USA: McGraw-Hill Education, 2019.

[51] V. Havary-Nassab, S. Shahbazpanahi, and A. Grami, "General-rank beamforming for multi-antenna relaying schemes," in *2009 IEEE International Conference on Communications*, June 2009, pp. 1–5.

[52] P. S. Tan, J. Paden, J. Li, J. Yan, and P. Gogineni, "Robust adaptive mvdr beamforming for processing radar depth sounder data," in *2013 IEEE International Symposium on Phased Array Systems and Technology*, Oct 2013, pp. 622–629.

[53] R. L. Haupt, *Antenna Arrays*. New York, NY, USA: John Wiley & Sons, Inc., 2010.

[54] D. Manolakis, V. K. Ingle, and S. M. Kogon, *Statistical and Adaptive Signal Processing: Spectral Estimation, Signal Modeling, Adaptive Filtering and Array Processing*. Artech House, 2005.

[55] Y. Yang and B. Jiao, "Information-guided channel-hopping for high data rate wireless communication," *IEEE Communications Letters*, vol. 12, no. 4, pp. 225–227, April 2008.

[56] T. Y. Elganimi and A. A. Elghariani, "Space-time block coded spatial modulation aided mmWave MIMO with hybrid precoding," in *2018 26th Signal Processing and Communications Applications Conference (SIU)*, May 2018, pp. 1–6.